Stockholm University

Ensembles and Open Quantum Systems in Polaritonic Chemistry

Eric Davidsson

Doctoral Thesis in Theoretical Physics at Stockholm University, Sweden 2023

Ensembles and Open Quantum Systems in Polaritonic Chemistry

Eric Davidsson

Academic dissertation for the Degree of Doctor of Philosophy in Theoretical Physics at Stockholm University to be publicly defended on Wednesday 31 May 2023 at 13.00 in Oskar Kleins auditorium (FR4), AlbaNova universitetscentrum, Roslagstullsbacken 21 and online via Zoom, public link is available at the department website.

Abstract

Optical cavities are structures where excitations in the electromagnetic field (photons of light) are confined and generally long-lived. The spatial confinement will enhance interactions with any matter systems in the cavity, such that the behaviour of a combined system is best understood in terms of polaritonic states; mixtures of excitations in both light and matter. This polaritonic regime provides a novel approach for the modification and control of chemical reactions, and a multitude of experimental advancements are beginning to realise this potential. There are however many challenges with creating useful theoretical models of the prominent quantum-mechanical behaviour in these systems, where model complexities regularly require numerical simulations.

In this thesis, we especially engage with two challenges from the field: One is to model cavities that contain ensembles of matter systems that interact collectively with the confined light. Another is to implement models based on open quantum systems, which is a dominant framework to include environment interactions.

With this work, we aim to deepen the understanding of the physics in these polaritonic chemistry systems. Our strategy is to isolate critical processes in order to study their significance and impact. In different contexts, this either allows us to identify potential obstacles to avoid or highlights opportunities to achieve desired experimental conditions and technological objectives.

Keywords: *Polaritonic Chemistry, Open Quantum Systems, Cavity QED, The Jaynes-Cummings Model, Optical Cavities, Computational Quantum Dynamics.*

Stockholm 2023
http://urn.kb.se/resolve?urn=urn:nbn:se:su:diva-216487

ISBN 978-91-8014-296-0
ISBN 978-91-8014-297-7

Department of Physics

Stockholm University, 106 91 Stockholm

ENSEMBLES AND OPEN QUANTUM SYSTEMS IN POLARITONIC CHEMISTRY

Eric Davidsson

Stockholm
University

Ensembles and Open Quantum Systems in Polaritonic Chemistry

Eric Davidsson

ISBN print 978-91-8014-296-0
ISBN PDF 978-91-8014-297-7

Printed in Sweden by Universitetsservice US-AB, Stockholm 2023

Abstract

Optical cavities are structures where excitations in the electromagnetic field (photons of light) are confined and generally long-lived. The spatial confinement will enhance interactions with any matter systems in the cavity, such that the behaviour of a combined system is best understood in terms of polaritonic states; mixtures of excitations in both light and matter. This polaritonic regime provides a novel approach for the modification and control of chemical reactions, and a multitude of experimental advancements are beginning to realise this potential. There are however many challenges with creating useful theoretical models of the prominent quantum mechanical behaviour in these systems, where model complexities regularly require numerical simulations.

In this thesis, we especially engage with two challenges from the field: One is to model cavities that contain ensembles of matter systems that interact collectively with the confined light. Another is to implement models based on open quantum systems, which is a dominant framework to include environment interactions.

With this work, we aim to deepen the understanding of the physics in these polaritonic chemistry systems. Our strategy is to isolate critical processes in order to study their significance and impact. In different contexts, this either allows us to identify potential obstacles to avoid or highlights opportunities to achieve desired experimental conditions and technological objectives.

Sammanfattning

Optiska kaviteter är strukturer där excitationer i det elektromagnetiska fältet (fotoner av ljus) kan fångas in och förbli långlivade. Som ett praktiskt exempel kan vi föreställa oss två parallella speglar som vetter mot varandra, där en ljuspuls studsar fram och tillbaka. Om vi placerar materiasystem (t.ex. atomer eller molekyler) mellan speglarna så kommer inneslutningen av ljuset att förstärka interaktionen mellan ljus och materia inne i kaviteten. Vi säger att vi är i en regim av *stark koppling*. I den här regimen beskrivs det kombinerade systemet bäst i termer av blandade tillstånd av både ljus och materia, så kallade *polaritontillstånd*. Här finns det nya möjligheter för att kontrollera och modifiera kemiska reaktioner, som än så länge inte har realiserats för några praktiska ändamål. Det är nämligen bara under de senaste 15 åren som kemiexperiment med stark ljus–materia koppling börjat bli vanliga, och vi utforskar fortfarande hur vi kan använda denna, så kallade, *polaritonkemi* till vår fördel.

Det finns emellertid många utmaningar med att konstruera bra teoretiska modeller för dessa system. De uppvisar nämligen ofta beteenden som bygger på de kvantmekaniska lagar som styr såväl materians minsta byggstenar som ljuset i kaviteten. Detta gör det fördelaktigt, eller ibland nödvändigt, att använda kvantmekaniska modeller. En annan komplikation är att system för polaritonkemi innehåller för många detaljer för att vi ska kunna göra beräkningar med analytiska metoder. I stället jobbar vi med numeriska metoder, som kan ge oss mycket bra svar och är flexibla nog för att hantera många av de frågor vi försöker besvara.

I den här uppsatsen fokuserar vi i synnerhet på två viktiga teoretiska utmaningar: En är att modellera optiska kaviteter som innehåller en hel ensemble av materiasystem, där alla delsystemen simultant interagerar med ljuset. En annan angelägen utmaning är modellera effekter som kommer av ytterligare interaktioner med en extern omgivning. Detta är modeller som bygger på så kallade *öppna kvantsystem*.

I båda fallen vill vi använda våra modeller för att fördjupa vår förståelse av fysiken som styr dessa polaritonkemisystem. Vår strategi är att separera ut centrala processer så att vi kan studera deras betydelse, en effekt i taget. Detta kan å ena sidan hjälpa oss att identifiera utmaningar på vägen mot att göra polaritonkemi användbart. Men förhoppningsvis också visa oss en väg framåt där vi identifierar användbara effekter av stark ljus–materia koppling. Antingen för experiment som ger oss nya insikter, eller för framtida teknologiska tillämpningar.

List of papers

Paper I

E. Davidsson and M. Kowalewski, "Atom Assisted Photochemistry in Optical Cavities", The Journal of Physical Chemistry A, vol. 124, no. 23, pp. 4672–4677, 2020. https://doi.org/10.1021/acs.jpca.0c03867. Open access. Cited as [1]. The paper is a reproduction with the permission of AIP Publishing.

Paper II

E. Davidsson and M. Kowalewski, "Simulating photodissociation reactions in bad cavities with the Lindblad equation", The Journal of Chemical Physics, vol. 153, no. 23, p. 234304, 2020. https://doi.org/10.1063/5.0033773. Open access. Cited as [2]. The paper is a reproduction with the permission of ACS Publications.

Paper III – Manuscript

E. Davidsson and M. Kowalewski, "The role of dephasing for dark state coupling in a molecular Tavis–Cummings model", 2023. https://doi.org/10.48550/arXiv.2304.09583. Cited as [3].

Author's contribution

Paper I

Title: "Atom assisted photochemistry in optical cavities".

I produced and analysed the data. Underlying quantum chemistry calculations were done by Prof. M. Kowalewski. I created code to manage parallel calculations on the Fugu cluster and to compile the results for analysis. I devised a method for distinguishing between avoided crossings and degenerate points along one-dimensional potential energy surfaces. The method was briefly discussed in the paper. I was the main contributor to writing the paper, except for the Introduction section where Prof. M. Kowalewski's contribution was more significant. I made an illustration that was selected for the supplementary cover.

Paper II

Title: "Simulating photodissociation reactions in bad cavities with the Lindblad equation".

I produced and analysed the data. I created Matlab/Octave code to run wave-packet simulations on excited states with the Lindblad equation. Underlying quantum chemistry calculations were done by Prof. M. Kowalewski. I created code to manage parallel calculations on the Fugu cluster and to compile the results for analysis. I devised a method to decrease the computational cost of time-evolution when using the Lindblad equation. A derivation and discussion of this method were included in a separate section in the appendix of the paper. I was the main contributor to writing the paper.

Paper III – Manuscript

Title: "The role of dephasing for dark state coupling in a molecular Tavis–Cummings model".

I produced and analysed the data. I did underlying quantum chemistry calculations on the CO molecule. I created code to manage parallel calculations on the Fugu cluster and to compile the results for analysis. Prof. M. Kowalewski implemented quantum trajectories in the in-house QDng package, and I implemented the same method in Matlab to compare results. I analysed the consequences of a phenomenological construction of dephasing operators and devised a scheme to show that the error was acceptable for our system. I was the main contributor to writing the paper.

Material from licentiate thesis

This thesis contains adapted material from my licentiate thesis, also titled "Ensembles and Open Quantum Systems in Polaritonic Chemistry" (February 3, 2021). Chapter 1 (Introduction) is a distant adaption. Chapter 2 (Theory and Methods) is a mix of adapted and new sections. Sections 2.2, 2.5, 2.7, 2.8, 2.9, 2.10, and 2.11 are adapted, while sections 2.1, 2.3, and 2.6 are new. Chapter 3 contains the same sections but is mostly new. The Appendix, Chapter A, is a close adaption.

Acknowledgements

I want to thank my awesome supervisor Markus Kowalewski for the trust and encouragement you have given me throughout the work. Your assistance and guidance have been invaluable, as have of course your insights into the field and the fascinating research questions within it. I extend my heartfelt appreciation to my assistant supervisor Åsa Larson for your support and my mentor Supriya Krishnamurthy for your constructive pep-talks. I also give my thanks to Jonas Larson, whose willingness to always answer my questions has been invaluable to our research. Gratitude then goes out to my co-workers in the group. Thank you all for making these years a great experience, and for providing a supportive and inspiring research environment. Last, gratitude with no end to my love and wife Kateryna Kovalchuk, for your unwavering understanding and patience with my theoretical physics obsession.

Contents

CHAPTER 1

Introduction to Polaritonic Chemistry

My work belongs to a sub-field within cavity quantum electrodynamics called *polaritonic chemistry* [4–10]. Here so-called *optical cavities* allow for strong light–matter interactions that can affect how atoms and molecules behave and interact. Such interactions are of course the field of chemistry, which has had a profound impact on our modern society.

Polaritonic chemistry is however an interdisciplinary field at the intersection between chemistry and physics. Where—generally speaking—the physics of light–matter interactions allow us to address questions of chemistry. So on the one hand, the field draws heavily on tools and techniques from quantum electrodynamics, which is a sub-field of physics. And on the other hand, we are ultimately concerned with understanding and controlling processes in the domain of chemistry. This then means that the community contains a wide variety of specialists in subjects relating to both disciplines.

In this chapter, we begin by introducing *optical cavities* (section 1.1), the fundamental technology of polaritonic chemistry that makes the aforementioned strong light–matter interaction possible. Into these cavities we add *emitters*, which are for instance atoms or molecules. We therefore discuss some popular choices of emitters for polaritonic chemistry, but also through a wider scope for related fields. Before getting into the technical weeds of modelling these systems (chapter 2) we finish this introduction by exploring some important experiments in the field and the prospect of future applications (section 1.2).

1.1 Building blocks and research questions

The groundwork for polaritonic chemistry was laid back in 1963 by E. T. Jaynes and F. W. Cummings [11]. They published a theory paper in order to "clarify the relationship between the quantum theory of radiation [...] and the semi-classical theory [...], and to apply some of the results thus obtained in a study of amplitude and frequency stability of the ammonia beam maser". It was however their model and its associated Hamiltonian that has proven to be a legacy contribution. The so-called Jaynes–Cummings model employs non-relativistic Quantum Mechanics and describes an atom as a two-level system (the simplest model of matter, based on only two states). The atom continuously interchanges energy with a quantised electromagnetic field, and the light–matter interaction is moulded by a so-called *optical cavity*.

These optical cavities can be designed in a number of ways, what they all have in common is their purpose; to manipulate electromagnetic field excitations (photons of light) such that the interaction between light and matter is amplified. Note that even though the name "optical cavity" seems to imply a restriction to visible light, in this thesis we will use the name more broadly, to mean a cavity with resonances in any part of the electromagnetic spectrum.

The simplest example of an optical cavity is to picture two planar mirrors facing each other. We can then imagine a pulse of light bouncing back and forth between these surfaces, and each time it passes by something, like an atom or a molecule, interactions can take place. This is, however, not an accurate depiction when distances between the mirrors grow smaller. It is then more accurate to solve for electromagnetic standing waves in the space between the mirrors, so-called *field modes*, which are spread out in the entire space between the mirrors and continuously interact with any atoms or molecules in the cavity.

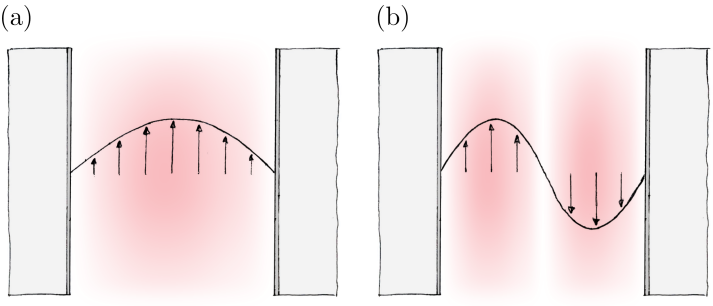

Figure 1.1: Schematic figure of planar optical cavities of the Fabry–Pérot type. The pink colour illustrates the field density in the electric field. (a) The fundamental mode (first harmonic) of the electric field. (b) The second harmonic of the electric field.

The planar, so-called, Fabry–Pérot cavity (figure 1.1) is commonly used and discussed in the literature [10]. It is however not the only type used for polaritonic chemistry. For instance, curving the mirrors inwards will give more long-lived mode excitations, as in a *confocal* cavity [12]. In fact, we can consider any arbitrary geometrical shape of reflective material. From a theoretical point of view, the resonant field modes can then be solved for numerically for an arbitrary cavity geometry.

Another structure that we also count as an optical cavity is the so-called *nano-plasmonic* cavity, though the physical principle behind this structure differs somewhat from the previous example. In short: If a metallic structure is exposed to an electric field, the free negative charges are slightly displaced relative to the positive ones. This creates a dipole expressed along the surface of the conductive material, and results in local concentrations in the electromagnetic field at particular points close to the surface. Since the charges also carry mass, and the dipole separation creates a restoring force, we can model this as an oscillator with a particular resonance frequency. Exposing this system to light that matches its resonance frequency will thus enhance the concentrating effect in the field. We can also let the metallic structure have dimensions on the nanoscale. Then the time-varying electric field is practically constant across the particle, and the entire structure becomes one single oscillating dipole. Some examples of these cavities are shown in figure 1.2.

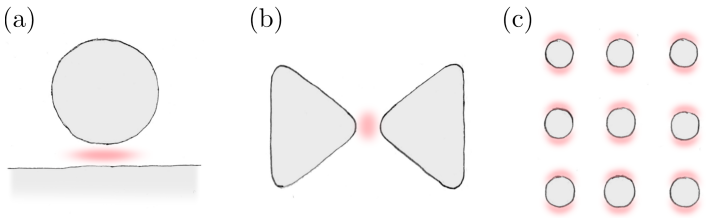

Figure 1.2: Schematic figures of three examples of plasmonic nano-cavities. The pink colour highlights relevant areas of field density concentrations. (a) A nano-sphere close to a metallic surface [10, 13, 14]. (b) A plasmonic bow tie antenna [15]. (c) A surface plasmonic lattice [8].

Note how the wavelengths of light in the Fabry–Pérot cavity (figure 1.1) are determined by the size of the cavity, but this is not so for a plasmonic cavity (figure 1.2). Since the resonance of the plasmonic cavity is determined by other properties, the available space is not as directly related to wavelength. Here it is, in fact, possible to have mode functions that are spatially smaller than the corresponding free-space wavelength of the electromagnetic oscillation [10].

Another difference worth pointing out is that the type of cavity with stand-

ing waves between reflective surfaces (figure 1.1) can typically accommodate a longer lifetime for the field excitations than the plasmonic nano-cavity (figure 1.2). Where in the latter, photon lifetimes are typically below 10 fs [10], and it may prove necessary to include decay effects in a model of the system.

We then want to introduce so-called *emitters* into the optical cavity, which are typically nanometre-sized, or smaller, material systems that interact with the electromagnetic field. In the papers in this thesis [1–3], emitters are either diatomic molecules or atoms, but other options will be addressed later in this section. The purpose of the cavity is to amplify the interaction between field and emitter when compared to, for instance, a standard free-space interaction. Figure 1.3 illustrates the resulting Jaynes–Cummings model, with a single atom as the emitter in a planar Fabry–Pérot cavity.

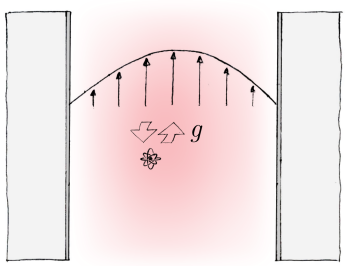

Figure 1.3: Schematic figure of the Jaynes–Cummings model. An atom is exchanging energy with the fundamental field mode in an optical Fabry–Pérot cavity. The light–matter interaction strength, g, is enhanced by the cavity. (The atom is not to scale.)

Currently, the systems that are both experimentally and theoretically studied under the umbrella of cavity quantum electrodynamics are modifications and evolutions of the original Jaynes–Cummings model. One branch of research is performed in the context of quantum information and quantum optics [16]. Another perspective is polaritonic chemistry—the topic of this thesis—where extensions of this system are interrogated for chemical effects and future applications [17]. Here, the Jaynes–Cummings model is modified by considering variations of either the atom or the electromagnetic field—or indeed both.

Regarding the cavity field, some examples from contemporary theoretical studies are, investigations of effects from polarization [18] and the number of included field modes [19]. Studying decay effects in the field is another avenue that is investigated in one of the papers in this thesis [2], and different types of cavities (as previously discussed) are analysed in terms of their pros and cons [15].

Regarding the emitter—which was a single atom in the Jaynes–Cummings model—the polaritonic chemistry literature encompasses many variations, such

as: organic dyes and pigments[1] [20], J-aggregates[2] [21, 22], and carbon nanotubes [23], but in principle, any molecule, small or large, is a potential emitter [24–28]. We can also take more examples from the wider subject of cavity quantum electrodynamics. Here we find emitters such as: excitons[3] in a crystalline material [29], quantum dots[4] [30] (review), superconducting qubits[5] [31] (review), and Bose-Einstein condensates[6] [29,32]. We also see systems that are formed from ensembles of the aforementioned systems [33, 34].

From the theoretical perspective, this diverse selection of emitters is modelled at different levels of theory depending on the demands of the study, and often what is computationally feasible. For chemistry purposes it is often beneficial, or even required, to include some quantum mechanical description of the nuclear dynamics. This fully quantum description of molecular vibrations is going to be the approach in all papers in this thesis [1–3].

Depending on the broader research direction, and what system is under study, there are various physical properties and observables that attract attention in the polaritonic chemistry literature. Some examples from the literature include electron transport [35, 36], isomerization[7] [25, 37], dissociation [1, 2], heat transfer [38], electron transfer [35], and vibrational spectra [24].

While the original Jaynes–Cummings model has an analytic solution [39], working with these extensions typically requires some numerical method. Extracting a phenomenological intuition from these models has been a challenge where the field has made significant advancements in recent decades. This development is spearheaded by advancements in high-performance computing.

[1] The colour of dyes and pigments comes from the strong absorption of specific wavelengths of visible light; due to excitations of valence electrons in pi-bond states.

[2] J-aggregates are string-like chains of aggregated dye molecules [21].

[3] Excitons are bound states of valence band electrons (in a solid-state material) that are attracted to a localised net positive charge.

[4] Quantum dots are semiconductor particles on the nanometre scale that despite their large size relative to atoms retains a similarly discrete energy spectrum.

[5] Superconducting qubit systems can be fabricated on chips and have, like all qubits, two relevant and distinct states. E.g. a Josephson junction that is made superconducting at low temperatures [31].

[6] Particles with a net zero spin, i.e. Bosons, have a permutation symmetric wavefunction. This allows for the global ground-state to be constructed from the individual ground-states of each particle. In this type of ground-state—a so-called Bose-Einstein condensate—the system exhibits some peculiar quantum mechanical phenomena.

[7] Isomerization is the process by which a molecule changes its geometric arrangement without swapping out any of the involved nuclei.

1.2 Experiments and applications

Though this thesis has a particular focus on the theoretical considerations in polaritonic chemistry, much of the activity in the field has been motivated and driven by advancements in experimental methods and results. A key experimental result was achieved in 1983 when, the 2012 Nobel prize winner, Serge Haroche together with Kaluzny, Goy, Gross, and Raimond, achieved a light–matter coupling that exceeded losses in the system [7,40]. They used an ensemble of sodium Rydberg atoms that traversed a microwave cavity. This experiment took cavity quantum electrodynamics into the so-called strong coupling regime (section 2.10), where the light–matter interactions are stronger than the losses in the system (such as photon decay). Shortly after, in 1985, Meschede, Walther, and Müller again achieved strong coupling in a microwave cavity, but this time for single atoms [41]. Another challenge was to demonstrate strong coupling for cavities resonant with visible light. This is particularly relevant for this thesis since our photon energies are in the ultraviolet, i.e. just outside visible light. Strong coupling with a cavity for visible light was achieved by Thompson, Rempe, and Kimble, in 1992 [42].

From the initial groundbreaking studies, experiments have branched out to encompass a multitude of different cavities and emitters (see discussion in the previous section 1.1). The experimental investigation into aspects of chemistry has, however, only been active for the past 15 years [8]. The range of research inquiries in cavity chemistry is broad, and includes topics such as relaxation dynamics from excited polaritonic states [43], the impact of the position of the emitters within the cavity [44], strong coupling to vibrational (not electronic) states [45], ground-state dissociation rate [46], energy transfer between types of molecules [47], showing coherent behaviour between molecular emitters [48], and many others [8].

However, despite these significant advances, there is still much to learn about the fundamental processes in these systems. For both experimental and theoretical studies, an initial desired objective is to be able to better understand, and thus predict, the behaviour in these systems. Having a good handle on how strong light–matter coupling generally influences chemical processes is a crucial aim for the field. For one thing, such knowledge will provide a toolkit for designing future research questions and experiments. But perhaps more important, we can then start designing practical applications, or perhaps in some instances, determine if some ideas are not feasible.

The exciting prospect of polaritonic chemistry is that we study a mechanism for influencing chemistry that has not yet been utilised for practical purposes. Thus, there may be revolutionary new ways to solve practical problems around the corner. A key aspiration is thus to establish strong light–matter coupling as a new mechanism for catalysing useful chemical reactions. However, getting to that point poses significant challenges. One such challenge, of a theoretical nature, is addressed ahead (section 3.1), while we focus on the practical

considerations in the present discussion.

One potential obstacle is the precision engineering and manufacturing of optical cavities for large-scale applications. While the kind of cavity relying on standing waves between reflective surfaces (figure 1.1) is potentially problematic for high-volume applications, the plasmonic cavity (figure 1.2) offers more flexibility for manufacturing and large-scale applications [10, 14]. However, these cavities can be constrained by their commonly short lifetimes of the electromagnetic excitations [10]. To the best of my knowledge, these practical challenges have not been systematically addressed. Thus, these considerations are the personal and speculative worries of a theorist.

Turning to the wider field of cavity quantum electrodynamics, the literature offers a diverse set of proposals for future applications. The opportunity to employ nanoscopic cavity structures to influence and control quantum phenomena on the single-particle scale invites applications in quantum information processing (QIP) [7, 49] as well as quantum computers [7, 50]. The mix of the spatial locality of the quantum emitters and the de-localised field modes suggests that cavities can be useful in quantum networks for computations [51, 52]. Accomplishing non-demolition measurements with these systems has been suggested as a route to interrogate the foundations of Quantum Mechanics [16, 51, 53] and studying decoherence in action [54]. And in relation to non-demolition measurements, cavity quantum electrodynamics may prove useful for high-precision quantum metrology [7].

CHAPTER 2

Theory and Methods

A common strategy to formulate a quantum mechanical model of charged particles interacting with the electromagnetic field starts with a classical description [55]. Unfortunately, even at this early point, there are different representations of Maxwell's famous equations [56], and choices along the way give different quantum mechanical descriptions [57]. In a landscape where even the most commonly walked paths are ceaselessly branching, this text does not set out to cover the subject exhaustively. We do, however, aim at giving the reader an example of the origin of the central equations, which are governing different system behaviours in polaritonic chemistry.

Along the way, we will point out a number of key strategies and concepts. We discuss for example: techniques for Maxwell's equations, such as gauge fixing, etc. (section 2.1), a light–matter interaction Hamiltonian (section 2.4), quantisation of an electromagnetic field (section 2.5), the Jaynes–Cummings model (sections 2.8 – 2.9), strong coupling (section 2.10), and open quantum systems (section 2.11). In addition to these rather foundational discussions, some numerical techniques are essential for the implementation of these models in day-to-day work. Thus, we also dip our toes into techniques for quantum chemistry (section 2.7).

2.1 Techniques for Maxwell's equations

Classical electrodynamics provides a good conceptual starting point for later generalisation to a quantum mechanical framework, the so-called *second quantisation* (section 2.5). The microscopic Maxwell's equations (where no medium is present) are a good starting point since we are building a model on the atomic length scale.

$$\begin{cases} \epsilon_0 \boldsymbol{\nabla} \cdot \mathbf{E} = \rho & \text{(2.1a)} \\ \dfrac{1}{\mu_0} \boldsymbol{\nabla} \times \mathbf{B} - \epsilon_0 \, \partial_t \mathbf{E} = \mathbf{J} & \text{(2.1b)} \\ \boldsymbol{\nabla} \cdot \mathbf{B} = 0 & \text{(2.1c)} \\ \boldsymbol{\nabla} \times \mathbf{E} + \partial_t \mathbf{B} = \mathbf{0} & \text{(2.1d)} \end{cases}$$

Here $\mathbf{E}(t, \mathbf{r})$ is the *electric* field, $\mathbf{B}(t, \mathbf{r})$ is the *magnetic* field, ϵ_0 is the electric *permittivity* of free space, μ_0 is the magnetic *permeability* of free space, $\rho(t, \mathbf{r})$ is the *charge density*, and $\mathbf{J}(t, \mathbf{r})$ is the *current density*.

The fields $\mathbf{E}$ and $\mathbf{B}$ have a special role because they are force fields; in the sense that the force experienced on some test-particle (with charge q and velocity $\mathbf{v}$) has a simple dependency on these fields. This relation is expressed by the *Lorentz force*, $\mathbf{F}$.

$$\mathbf{F} = q\big(\mathbf{E} + \mathbf{v} \times \mathbf{B}\big) \tag{2.2}$$

2.1.1 Potentials

An advantage of expressing Maxwell's equations in this form from equations (2.1), is that the Lorenz force, from equation (2.2), provides a relatively intuitive interpretation of the theory. There are however some generally undesirable features. As independent mathematical objects, the vector fields, $\mathbf{E}(t, \mathbf{r})$ and $\mathbf{B}(t, \mathbf{r})$, correspond to six degrees of freedom at each space-time point. However, Maxwell's equations (2.1) constrain the allowed configurations so that the total number of degrees of freedom is, in fact, fewer than six. Put differently, using $\mathbf{E}$ and $\mathbf{B}$ to specify the state is an over-specification, and in the following, we shall demonstrate how to replace these state variables with a different construction that has the constraints built in.

Since the $\rho(t, \mathbf{r})$ and $\mathbf{J}(t, \mathbf{r})$, in equations (2.1a) and (2.1b), are arbitrary functions, we instead focus on the two homogeneous equations, (2.1c) and (2.1d). We intend to fulfil them no matter what, by building them into the very state description. Equation (2.1c) says that $\mathbf{B}$ has no divergence (i.e. the absence of magnetic charges). To fulfil this condition, we can construct a vector field, $\mathbf{A}(t, \mathbf{r})$, with the property that taking its curl will give us the intended magnetic field, $\mathbf{B}$.

$$\mathbf{B} =: \boldsymbol{\nabla} \times \mathbf{A} \tag{2.3}$$

This makes sure that equation (2.1c) is fulfilled, since the curl of any vector field always has zero divergence, i.e. $\boldsymbol{\nabla} \cdot \boldsymbol{\nabla} \times \mathbf{A} = 0 \ \forall \, \mathbf{A}$. We insert equation (2.3) in our second homogeneous equation (2.1d) and exchange the order of curl and time derivative.

$$\boldsymbol{\nabla} \times \big(\mathbf{E} + \partial_t \mathbf{A} \big) = 0 \tag{2.4}$$

Since the above parenthesis evidently has no curl, it is by definition a conservative vector field, which can always be expressed as the gradient of some appropriate potential. We call that potential $\Phi(t, \mathbf{r})$.

$$\mathbf{E} + \partial_t \mathbf{A} =: -\boldsymbol{\nabla} \Phi \tag{2.5}$$

$$\Rightarrow$$

$$\mathbf{E} = -\boldsymbol{\nabla} \Phi - \partial_t \mathbf{A} \tag{2.6}$$

With the two equations (2.3) and (2.6) we can calculate $(\mathbf{E}, \mathbf{B})$ from $(\Phi, \mathbf{A})$, and we have ensured that whatever Φ and $\mathbf{A}$ are, the equations (2.1c) and (2.1d) are fulfilled. The original four Maxwell's equations can thus be collapsed to only two, for Φ and $\mathbf{A}$.

$$\begin{cases} -\partial_t \big(\boldsymbol{\nabla} \cdot \mathbf{A} \big) - \nabla^2 \Phi = \dfrac{\rho}{\epsilon_0} & \text{(2.7a)} \\ \Box^2 \mathbf{A} + \boldsymbol{\nabla} \left(\boldsymbol{\nabla} \cdot \mathbf{A} + \dfrac{1}{c^2} \partial_t \Phi \right) = \mu_0 \mathbf{J} & \text{(2.7b)} \end{cases}$$

Here, the box, $\Box^2$, is the d'Alembertian, whose homogeneous solutions are propagating waves.

$$\Box^2 := \frac{1}{c^2} \partial_t^2 - \nabla^2 \tag{2.8}$$

The equations in (2.7) do however still contain some non-trivial arbitrariness, in the sense that there are particular ways to change Φ and $\mathbf{A}$ such that our physical force fields $\mathbf{E}$ and $\mathbf{B}$ remain unaffected. This is the so-called *gauge freedom*. Gauge fixing, i.e. removing the gauge freedom by imposing some artificial constraint on Φ and $\mathbf{A}$, can simplify the equations in (2.7). How we make that choice depends on the intended application, where particular *gauges* will suit specific problems.

Since equation (2.3) defines $\mathbf{A}$ such that $\mathbf{B}$ is the curl of $\mathbf{A}$, we can add a vector field with zero curl to $\mathbf{A}$ without affecting $\mathbf{B}$. If interpreted as a force field, a vector field with zero curl is conservative, and can always be described as the gradient of some scalar potential, which we will call $\Lambda(t, \mathbf{r})$. Thus, $\mathbf{B}$ will not be affected by the following transformation, irrespective of how we chose the arbitrary function Λ.

$$\mathbf{A} \to \mathbf{A}' = \mathbf{A} + \boldsymbol{\nabla} \Lambda \tag{2.9}$$

Inserting this into equation (2.6), we find that the potential Φ is correspondingly

transformed by any time derivative of Λ.

$$\Phi \to \Phi' = \Phi - \partial_t \Lambda \tag{2.10}$$

Thus it turns out that the freedoms in $\mathbf{A}$ are the spatial derivatives of Λ, and the freedom in Φ is the temporal derivative.

2.1.2 Longitudinal and transverse fields

According to Helmholtz's decomposition theorem, any sufficiently smooth, and fast enough decaying, vector field, $\mathbf{W}$, can be uniquely split into two fields, each with its defining attribute. One is a vector field with zero curl, $\mathbf{W}^{||}$, which we call the *longitudinal* field (also known as *irrotational*). The other is a vector field with zero divergence, $\mathbf{W}^{\perp}$, and we call it the *transverse* field (also known as *solenoidal*).

$$\mathbf{W} = \mathbf{W}^{||} + \mathbf{W}^{\perp} \qquad \text{where} \qquad \boldsymbol{\nabla} \times \mathbf{W}^{||} = \mathbf{0} \qquad \text{and} \qquad \boldsymbol{\nabla} \cdot \mathbf{W}^{\perp} = 0 \tag{2.11}$$

Note how these definitions imply that the magnetic field, $\mathbf{B}$, is purely transversal. See equation (2.1c)

2.1.3 Lorenz gauge

A commonly occurring choice of gauge is the so-called Lorenz Gauge. For quantum chemistry and cavity electrodynamics, this is not the preferred choice of gauge, and we only mention it briefly as an example of a possible choice with some nice properties. Here we demand that the a term from (2.7b) must vanish.

$$\boldsymbol{\nabla} \cdot \mathbf{A} + \frac{1}{c^2} \partial_t \Phi = 0 \tag{2.12}$$

In the interest of brevity, we will not show that this is indeed possible within our gauge freedom. The result is that the equations (2.7) transform into a set of symmetric and decoupled equations whose Lorentz invariance makes them particularly useful for relativistic applications.

$$\begin{cases} \Box^2 \Phi = \dfrac{\rho}{\epsilon_0} & \text{(2.13a)} \\ \Box^2 \mathbf{A} = \mu_0 \mathbf{J} & \text{(2.13b)} \end{cases}$$

2.1.4 Coulomb gauge

The so-called Coulomb gauge—which is also referred to as *transverse* or *radiation* gauge [58]—is another popular option. Comparing to equation (2.12),

here we only demand that the divergence of $\mathbf{A}$ vanishes.

$$\boldsymbol{\nabla} \cdot \mathbf{A} = 0 \tag{2.14}$$

This is accomplished by splitting some initial $\tilde{\mathbf{A}}$ into transverse and longitudinal components and setting the latter $\tilde{\mathbf{A}}^{||} = \mathbf{0}$. With this condition, we rewrite the equations in (2.7).

$$\begin{cases} -\nabla^2 \Phi = \dfrac{\rho}{\epsilon_0} & \text{(2.15a)} \\ \Box^2 \mathbf{A} + \dfrac{1}{c^2} \boldsymbol{\nabla}\big(\partial_t \Phi\big) = \mu_0 \mathbf{J} & \text{(2.15b)} \end{cases}$$

This may not look as symmetric and aesthetically pleasing as equations (2.13), but a nice property here is the simple interpretation of the scalar potential, Φ. Equation (2.15a) is the Poisson equation, and its solution reproduces the electric potential due to a charge distribution [59].

$$\Phi(t, \mathbf{r}) = \frac{1}{4\pi\epsilon_0} \int \frac{\rho(t, \mathbf{r}')}{|\mathbf{r} - \mathbf{r}'|} \, \mathrm{d}^3 r' \tag{2.16}$$

In other words, $\Phi(t, \mathbf{r})$ is here the potential used in Coulomb's law, hence the name of this gauge.

In the Coulomb gauge, since $\mathbf{A}$ has no divergence it is a purely transversal field, and the definition of the electric field from equation (2.6) can be split up into simpler relations for the transverse and longitudinal components.

$$\begin{cases} \mathbf{E}^{||} = -\boldsymbol{\nabla}\Phi & \text{(2.17a)} \\ \mathbf{E}^{\perp} = -\partial_t \mathbf{A} & \text{(2.17b)} \\ \mathbf{B} \;\; = \boldsymbol{\nabla} \times \mathbf{A} & \text{(2.17c)} \end{cases}$$

For completeness, the magnetic field from equation (2.3) is also included.

2.1.5 The long wavelength limit

The long wavelength limit [56], which can also be referred to as the *dipole approximation* [55], is perhaps more accurately the single-particle version of the dipole approximation.

We can successfully apply the long wavelength limit where the spatial size of the particle is much smaller than the wavelength of the relevant electromagnetic radiation. As a practical example, we can take the situation in the papers in this thesis; where a molecule is interacting with ultraviolet light. The size of the molecule is on the order of 10^{-1} nm, while the wavelength of the light is on the order of 10^{2} nm.

To demonstrate this approximation, we start by considering a free-space

solution to Maxwell's equations (2.15) for Φ and $\mathbf{A}$, in the Coulomb gauge. Free space implies that there are no charges or currents around, so $\rho = 0$ and $\mathbf{J} = \mathbf{0}$. In solving the equations in some arbitrary cubic volume L^3, with no charges around we can set the electric potential on the boundary to be zero. Then, according to equation (2.15a), $\Phi = 0$ in the volume. The equations (2.15) thus collapse to the homogeneous wave-equation for $\mathbf{A}$ [60].

$$\Box^2 \mathbf{A} = \mathbf{0} \tag{2.18}$$

The solution to this is the free-space radiation, which is a superposition of plane waves, $\mathrm{e}^{\mathrm{i}\,\mathbf{k}\cdot\mathbf{r}}$, linearly polarized along the two unit vectors $\mathbf{n}_{\mathbf{k}}^{(1)}$ and $\mathbf{n}_{\mathbf{k}}^{(2)}$, both perpendicular to $\mathbf{k}$.

$$\mathbf{A}(t,\mathbf{r}) = \sum_{\mathbf{k},\lambda} \mathbf{n}_{\mathbf{k}}^{(\lambda)} \Big(q_{\mathbf{k}}(t)\, \mathrm{e}^{\mathrm{i}\,\mathbf{k}\cdot\mathbf{r}} + q_{\mathbf{k}}^{*}(t)\, \mathrm{e}^{-\mathrm{i}\,\mathbf{k}\cdot\mathbf{r}} \Big) \quad \text{where} \quad \mathbf{n}_{\mathbf{k}}^{(\lambda)} \cdot \mathbf{k} = 0 \tag{2.19}$$

Inserting this back into equation (2.18) allows us to determine the time-varying complex amplitudes, $q_{\mathbf{k}}(t)$ and $q_{\mathbf{k}}^{*}(t)$, which can be selected to give real solutions. If considering a particular mode, $\mathbf{k}$, and linearly polarized light along the unit vector $\mathbf{n}$, we can simplify the solution [55].

$$\mathbf{A}(t,\mathbf{r}) = \mathbf{n}\, Q \cos\big(\mathbf{k}\cdot\mathbf{r} - \omega t + \phi\big) \quad \text{where} \quad \mathbf{n}\cdot\mathbf{k} = 0 \tag{2.20}$$

Such waves travel at the speed of light, since $\omega = |\mathbf{k}|c$, and this will be sufficient for the discussions in the following sections.

In the long wavelength limit we argue that if we only care about the interaction of an emitter, the spatial modulation far from the emitter is irrelevant. Additionally, because of the difference in scale (between the emitter and the wavelength of the light), the field has only a negligible change across the emitter. Thus, we replace the spatially modulated plane waves, $\mathbf{A}(t,\mathbf{r})$, from equation (2.20), with a time-varying constant throughout space, $\mathbf{A}(t)$.

$$\mathbf{A}(t) = \mathbf{n}\, Q \cos\big(\omega t + \phi\big) \tag{2.21}$$

2.2 Quantisation

Ordinarily, the quantisation of a classical theory starts with an operator commutation relation [60], such as $[\hat{x}, \hat{p}] = \mathrm{i}\hbar\hat{\mathbb{1}}$. However, this presentation can easily obfuscate how the transition into a new mathematical framework occurred. Here we start with this conceptual transformation, and the commutation relation is a consequence we could derive.

In the quantum mechanical framework, the Schrödinger equation is central for describing the time-evolution of any (isolated) system.

$$\mathrm{i}\hbar\partial_t \left|\psi\right\rangle = \hat{H} \left|\psi\right\rangle \tag{2.22}$$

In this section, we give a quick outline of the mathematical objects above, and in particular, how to transform a known classical Hamiltonian to a quantum mechanical operator, $\hat{H}$. In the next section 2.3, we will apply this recipe to the minimal coupling Hamiltonian, and then again to the cavity field, in section 2.5.

Transforming a classical description into the framework for non-relativistic quantum theory is to move the mathematical model of point particles and densities to a problem in functional analysis: Instead of giving a particle a real-valued, and independent, position and momentum, $\mathbf{r}(t)$ and $\mathbf{p}(t)$, we start by promoting each position $\mathbf{r} \in \mathbb{R}^3$, to be a state of the system, $\{|\mathbf{r}\rangle\}$. To connect such states with their initial coordinates, we introduce an *operator*, $\hat{\mathbf{r}}$, that will give the coordinates back when operating on the position eigenstates.

$$\hat{\mathbf{r}} \left|\mathbf{r}\right\rangle = \mathbf{r} \left|\mathbf{r}\right\rangle \qquad \text{with} \qquad \mathbf{r} \in \mathbb{R}^3 \tag{2.23}$$

The states $\{|\mathbf{r}\rangle\}$ are then used to span a complex vector space, $\mathfrak{H}$, containing all allowed states of the system. A significant consequence of this move is that any complex superposition of $\{|\mathbf{r}\rangle\}$ is also an allowed state of the system.

$$\int_{\mathbf{r}} \left|\mathbf{r}\right\rangle \psi(\mathbf{r}) \,\mathrm{d}^3 r \;\in\; \mathfrak{H} \tag{2.24}$$

Here, $\psi(\mathbf{r})$ is a complex-valued density referred to as the wavefunction. We can consider this complex density to be a projection of a more mathematically abstract *state*, $|\psi\rangle$, on the position basis $\{|\mathbf{r}\rangle\}$, i.e. $\psi(\mathbf{r}) = \langle\mathbf{r}|\psi\rangle$.

$$\int_{\mathbf{r}} \left|\mathbf{r}\right\rangle \left\langle\mathbf{r}|\psi\right\rangle \,\mathrm{d}^3 r = \left(\int_{\mathbf{r}} \left|\mathbf{r}\right\rangle\!\left\langle\mathbf{r}\right| \mathrm{d}^3 r\right) \left|\psi\right\rangle \tag{2.25}$$

In the second step we have separated the basis projection (in the above parenthesis), from the state, $|\psi\rangle$, which is a member of the vector space, i.e. $|\psi\rangle \in \mathfrak{H}$.

To encode momentum in this framework, we use the rotation of the wavefunction in the complex plane; where twisting the wavefunction in the complex plane imparts momentum to the state. Expressed differently, and with some mathematical rigour, we let the Fourier transform of the wavefunction, $\psi(\mathbf{r})$, be the conjugate wavefunction, $\tilde{\psi}(\mathbf{k})$, in the momentum basis $\{|\mathbf{k}\rangle\}$ (where Plank's constant converts into units of momentum: $\mathbf{p} = \hbar\mathbf{k}$).

$$\tilde{\psi}(\mathbf{k}) = \frac{1}{(2\pi)^{3/2}} \int_{\mathbf{r}} \psi(\mathbf{r})\, \mathrm{e}^{-\mathrm{i}\mathbf{k}\cdot\mathbf{r}}\, \mathrm{d}^3 r \tag{2.26}$$

A useful interpretation of the above Fourier transform is as a projection onto the eigenfunctions of momentum. This implies that for some particular $\mathbf{k}$, we should think of $f(\mathbf{r}) = \mathrm{e}^{-\mathrm{i}\mathbf{k}\cdot\mathbf{r}}$ as a (non-normalizable) eigenfunction of momentum, expressed in the position basis $\{|\mathbf{r}\rangle\}$. Defining an operator, analogous to equation (2.23), which gives the momentum of $\mathrm{e}^{-\mathrm{i}\mathbf{k}\cdot\mathbf{r}}$ is then fairly straightforward—since taking the spatial derivative will bring down the wavenumber, $\mathbf{k}$, from the exponential.[1]

$$\hat{\mathbf{p}} := -\mathrm{i}\hbar\hat{\boldsymbol{\nabla}}_{\mathbf{r}} \tag{2.27}$$

In the interest of full disclosure, we can borrow the basis projection from equation (2.25) to declare the basis in which equation (2.23) and (2.27) applies.

$$\begin{cases} \hat{\mathbf{r}} = \displaystyle\int_{\mathbf{r}} \mathbf{r}\, |\mathbf{r}\rangle\langle\mathbf{r}|\, \mathrm{d}^3 r & \text{(2.28a)} \\ \hat{\mathbf{p}} = -\mathrm{i}\hbar \displaystyle\int_{\mathbf{r}} \boldsymbol{\nabla}_{\mathbf{r}}\, |\mathbf{r}\rangle\langle\mathbf{r}|\, \mathrm{d}^3 r & \text{(2.28b)} \end{cases}$$

Choice of basis is however often implied, and since this notation is somewhat cumbersome it is rarely used in the literature relevant to this thesis.

As a final point, note that we have implicitly assumed that we can take inner products in this complex vector space, $\mathfrak{H}$. We accomplish this by associating the vector space with a *sesquilinear*[2] inner product. Since any vector space with an associated inner product composes a so-called *Hilbert space*, will use this term for $\mathfrak{H}$ going forward.

[1] Note how radical this change is. Before quantisation, momentum was characterised by how point particles change their positions *with time*, and the new idea is to represent momentum by how a function is changing in *space*.

[2] The term *sesquilinear* refers to the fact that the inner product is ordered and picks up a complex conjugation when swapped: $\langle\psi_1|\psi_2\rangle = \langle\psi_2|\psi_1\rangle^*$. By conversion, in quantum theory, the first argument contains the complex conjugation when a vector is multiplied by a number: $\langle\alpha\psi_1|\psi_2\rangle = \alpha^* \langle\psi_1|\psi_2\rangle$, but $\langle\psi_1|\alpha\psi_2\rangle = \alpha \langle\psi_1|\psi_2\rangle$.

2.3 The minimal coupling Hamiltonian

The dynamics of a classical particle with charge q in an electrodynamic field is described by the minimal coupling Hamiltonian.

$$H = \frac{1}{2m}\big(\mathbf{p} - q\mathbf{A}\big)^2 + q\Phi \tag{2.29}$$

One can show that this minimal coupling Hamiltonian will reproduce the Lorentz force from equation (2.2) [55].

2.3.1 The first quantisation

A classical Hamiltonian can then be *quantised*—following the argument from section 2.2—by replacing classical quantities with their Hilbert-space operator counterpart. In the case of the minimal coupling Hamiltonian from equation (2.29) we replace $\mathbf{p}$ with the operator, $\hat{\mathbf{p}}$, from equation (2.27).

$$\hat{H} = \frac{1}{2m}\big(\hat{\mathbf{p}} - q\mathbf{A}(t, \hat{\mathbf{r}})\big)^2 + q\Phi(t, \hat{\mathbf{r}}) \tag{2.30}$$

In addition, we of course also adopt Hilbert space vectors for describing states.

In equation (2.30), we omit hats on $\mathbf{A}$ and Φ to denote the fact that the fields are still treated classically. In section 2.5 we will proceed with a second quantisation of fields, but for now, we proceed with this semi-classical minimal coupling Hamiltonian.

The result in equation (2.30) can also be derived from an underlying Lagrangian framework [59], something we will not entertain here. Though equation (2.30) includes some magnetic interactions, it lacks others. We discuss this in more detail in section 2.6.

2.3.2 Fixing to the Coulomb gauge

The light–matter interaction Hamiltonian that we will derive in this section is based on the quantised minimal coupling Hamiltonian (section 2.3.1), fixes the gauge according to the Coulomb gauge (section 2.1.4), and employs the long-wavelength limit (section 2.1.5).

To expose the consequences of the gauge fixing, we start by inserting the explicit particle momentum, $\hat{\mathbf{p}} := -\mathrm{i}\hbar\hat{\boldsymbol{\nabla}}_{\mathbf{r}}$, in equation (2.30), and expand the square (remembering that $\hat{\boldsymbol{\nabla}}_{\mathbf{r}}$ is a total derivative of everything with an $\mathbf{r}$ dependence to its right).

$$\hat{H} = \frac{1}{2m}\left(-\hbar^2\hat{\nabla}_{\mathbf{r}}^2 + \mathrm{i}\hbar q(\hat{\boldsymbol{\nabla}}_{\mathbf{r}}\cdot\mathbf{A}) + \mathrm{i}\,2\hbar q\mathbf{A}\cdot\hat{\boldsymbol{\nabla}}_{\mathbf{r}} + q^2\mathbf{A}^2\right) + q\Phi \tag{2.31}$$

The Coulomb gauge sets the divergence of $\mathbf{A}$ to zero, as seen in equation (2.14), which removes one term from equation (2.31).

$$\hat{H} = \frac{1}{2m}\left(-\hbar^2\hat{\nabla}_{\mathbf{r}}^2 + \mathrm{i}2\hbar q\mathbf{A}\cdot\hat{\boldsymbol{\nabla}}_{\mathbf{r}} + q^2\mathbf{A}^2\right) + q\Phi \tag{2.32}$$

Specified by $\mathbf{A}(t,\hat{\mathbf{r}})$, a phase is extracted from the wave function $\psi'(t,\hat{\mathbf{r}})$, and we get a new wavefunction $\psi'(t,\hat{\mathbf{r}})$. This move will eventually simplify the Hamiltonian.

$$\psi(t,\hat{\mathbf{r}}) = \mathrm{e}^{\mathrm{i}\,q(\hat{\mathbf{r}}\cdot\mathbf{A})/\hbar}\,\psi'(t,\hat{\mathbf{r}}) \tag{2.33}$$

We can rewrite the Schrödinger equation to work with the new wavefunction, $\psi'(t,\hat{\mathbf{r}})$, and this transforms the time derivative and operators in the Hamiltonian as follows. See the appendix, section A.1.1, for the details of this calculation.

$$\begin{cases} \mathrm{i}\hbar\partial_t \to \mathrm{i}\hbar\partial_t - q\big(\hat{\mathbf{r}}\cdot\partial_t\mathbf{A}\big) & \text{(2.34a)} \\ \hat{\boldsymbol{\nabla}}_{\mathbf{r}} \to \hat{\boldsymbol{\nabla}}_{\mathbf{r}} + \dfrac{\mathrm{i}q}{\hbar}\mathbf{A} & \text{(2.34b)} \\ \hat{\nabla}_{\mathbf{r}}^2 \to \hat{\nabla}_{\mathbf{r}}^2 + \dfrac{\mathrm{i}2q}{\hbar}\mathbf{A}\cdot\hat{\boldsymbol{\nabla}}_{\mathbf{r}} - \dfrac{q^2}{\hbar^2}\mathbf{A}^2 & \text{(2.34c)} \end{cases}$$

This is inserted into the Schrödinger equation based on our Hamiltonian from equation (2.32), and the expression is simplified, see the appendix section A.1.2. Since from now on we are only working with the new wavefunction ψ', we can drop the prime.

$$\mathrm{i}\hbar\partial_t\psi(t,\mathbf{r}) = \left(\frac{-\hbar^2}{2m}\hat{\nabla}_{\mathbf{r}}^2 + q\Phi + q\big(\hat{\mathbf{r}}\cdot\partial_t\mathbf{A}\big)\right)\psi(t,\mathbf{r}) \tag{2.35}$$

In the Coulomb gauge the time derivative of $\mathbf{A}$ is the transversal electric field, see equation (2.17b).

$$\mathrm{i}\hbar\partial_t\psi(t,\mathbf{r}) = \left(\frac{-\hbar^2}{2m}\hat{\nabla}_{\mathbf{r}}^2 + q\Phi - q\big(\hat{\mathbf{r}}\cdot\mathbf{E}^{\perp}\big)\right)\psi(t,\mathbf{r}) \tag{2.36}$$

We then have our minimal coupling Hamiltonian in the Coulomb gauge.

$$\hat{H} = \frac{-\hbar^2}{2m}\hat{\nabla}_{\mathbf{r}}^2 + q\Phi - q\big(\hat{\mathbf{r}}\cdot\mathbf{E}^{\perp}\big) \tag{2.37}$$

When compared to our starting point in equation (2.31), this looks considerably simpler. What this Hamiltonian still lacks is energy stored in the field itself. We will correct this omission in section 2.5.

Only the last term in equation (2.37) now contains both field and the particle degrees-of-freedoms, thus it is our interaction Hamiltonian, $\hat{H}_{\mathrm{int}}$. Keeping

in mind that this Hamiltonian relates to the transverse field, it is customary to drop the signifier.

$$\hat{H}_{\text{int}} = -q\big(\hat{\mathbf{r}} \cdot \mathbf{E}\big) \tag{2.38}$$

In the next section, 2.5, we are going to quantise this transverse electric field.

2.4 Sketching a multi-particle generalization and the dipole approximation

The discussion so far has related to a single particle, but both atoms and molecules are of course many-body systems. We can however generalise the minimal coupling Hamiltonian, in equation (2.30), by summing over the individual particle momenta and adding Coulomb interactions (longitudinal electric fields) between all pairs or particles. If, as before (section 2.1.5), we assume no external charges then $\Phi = 0$.

$$\hat{H} = \sum_i \frac{1}{2m_i}\big(\hat{\mathbf{p}}_i - q_i\mathbf{A}(t,\hat{\mathbf{r}}_i)\big)^2 + \frac{1}{4\pi\epsilon_0}\sum_{i<j}\frac{q_i q_j}{|\hat{\mathbf{r}}_i - \hat{\mathbf{r}}_j|} \tag{2.39}$$

It is however rarely desirable to work with absolute coordinates, so we transform the positions of the particles into a set of relative coordinates, for instance using the particles' centre of mass.

The interaction terms between $\hat{\mathbf{p}}_i$ and $\mathbf{A}$ will create a complicated mess when we change the coordinates [60]. However, one can introduce approximations that will simplify those equations. This is a detailed process that we will only briefly outline here, see for instance [57, 59, 60] for further details.

Initially, each particle has an interaction term with the electric field, as derived in equation (2.38). We then Taylor expand $\mathbf{A}(t,\mathbf{x})$ around a point, and we will find that a term with $\mathbf{E}(t)$, which is time-varying but constant throughout space, interacts with the total dipole of the set of particles, $\hat{\mathbf{d}}$.

$$\hat{H}_{\text{int}} = -\hat{\mathbf{d}}\cdot\mathbf{E}(t) \qquad \text{where} \qquad \hat{\mathbf{d}} := \sum_{n=1}^{N} q_n\hat{\mathbf{r}}_n \tag{2.40}$$

Consequently, we are in a multi-particle regime of the long wavelength limit (section 2.1.5). This regime is referred to as the *dipole approximation*.

2.5 Cavity fields and the second quantisation

When quantising the free field, a classical field is divided into the uncountably infinite set of all propagation vectors, $\{\mathbf{k}\}$. Such *field modes* are plane waves that are maximally spread out in space. For any mode $\mathbf{k}'$, the energy in the field grows quadratically as a function of the amplitude. This results in a harmonic potential where particular amplitude superpositions form eigenstates with equally spaced energies. These amplitude eigenstates are then identified as the photons in the field. In the case of a field confined to an optical cavity, the procedure is similar, but it simplifies since the set of propagation vectors, $\{\mathbf{k}\}$, is only countably infinite. Here is how this is done:

For the coming quantisation, we consider a minimal model in the Coulomb gauge (section 2.1.4) with a simplified *cavity mode shape*, i.e. how the field strength is geometrically arranged and falls off towards open or conducting boundaries. Consider an optical cavity, from two planar mirrors, with the z-axis perpendicular to the surfaces. See figure 2.1.

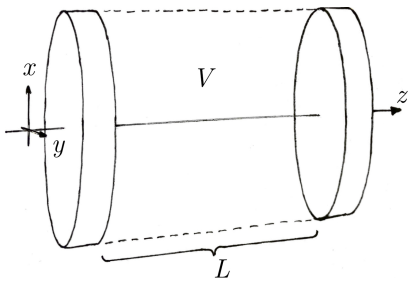

Figure 2.1: Model of a box with parallel mirrors. The z-axis lies along the cavity. The length of the cavity is L, and the enclosed volume between the mirrors is V.

In this optical cavity, we look for a classical field solution for a time-varying field along the z-axis, $\mathbf{A}(t, z)$ and $\Phi(t, z)$. In any x-y plane, the field is assumed to be constant inside the cavity and zero outside. This is of course a rather unphysical approximation, however, as is shown in the appendix, section A.2, this only affects the scalar result from the evaluation of a volume integral. Thus we can use this simple model to illustrate how the same Hamiltonian is constructed also for more geometrically realistic scenarios.

We repeat the argument in section 2.1.5 to recognize that we again need to solve the homogeneous wave-equation $\Box^2\mathbf{A} = \mathbf{0}$. From equation (2.20) we want to select equal superpositions of waves travelling in opposite directions ($\mathbf{e}_z$ and $-\mathbf{e}_z$) such that nodes of $\mathbf{A}$ intersect with the mirror boundaries.[3] For this, the

[3] From equations (2.17), we see that for the electric field, $\mathbf{E}^\perp$, to vanish along the conducting boundary we need $\partial_t\mathbf{A} = \mathbf{0}$. This only happens if a node intersects with the boundary.

wave vector has to be restricted to multiples of the cavity length, and without loss of generalisation, we introduce a restriction to polarised light along $\mathbf{e}_x$.

$$\begin{gathered}\mathbf{A}_n(t,z) = \mathbf{e}_x\, Q(t)\sin(k_n z) \\ \text{where} \\ k_n = \frac{\omega_n}{c} = \frac{\pi n}{L} \quad ; \quad n \in \mathbb{N}_1 \quad ; \quad z \in [0, L]\end{gathered} \tag{2.41}$$

In the following, we will quantise each mode k_n independently. Once the field is quantised we can re-introduce superpositions in the quantum mechanical framework. Note, due to the direct relationship between the k_n and ω_n, the latter is actually more commonly used to characterise modes.

Like with the minimal coupling Hamiltonian from section 2.3, we start with the classical Hamiltonian, which gives the energy of a field configuration of $\mathbf{E}$ and $\mathbf{B}$.

$$H = \frac{\epsilon_0}{2}\int_V \mathbf{E}^2 + c^2\mathbf{B}^2 \,\mathrm{d}V \tag{2.42}$$

Using the Coulomb gauge recipe from equations (2.17), we can get $\mathbf{E}$ and $\mathbf{B}$ from $\mathbf{A}$ in equation (2.41).

$$\begin{cases}\mathbf{E}_n^{\perp}(t,z) = \mathbf{e}_x\sqrt{\dfrac{2}{\epsilon_0 V}}\,(\partial_t q)\sin(k_n z) \\ \mathbf{B}_n(t,z) = \mathbf{e}_y\, k_n\sqrt{\dfrac{2}{\epsilon_0 V}}\, q(t)\cos(k_n z)\end{cases} \tag{2.43}$$

$$\begin{gathered}\text{where} \\ k_n = \frac{\omega_n}{c} = \frac{\pi n}{L} \quad ; \quad n \in \mathbb{N}_1 \quad ; \quad z \in [0, L]\end{gathered}$$

Note that we have pulled a constant out of the amplitude from equation (2.41), like this:

$$Q(t) = \sqrt{\frac{2}{\epsilon_0 V}}\, q(t) \tag{2.44}$$

Here, V is the total volume of the cavity, more generally known as the *effective mode volume* [60] for arbitrary spatial mode shapes. There are two reasons for this constant, each associated with its own factor. The first factor, $\sqrt{2/V}$, comes from a normalisation requirement on the mode functions [60]. The second factor, $\sqrt{1/\epsilon_0}$, gives $q(t)$ the appropriate units in preparation for the canonical quantisation of $q(t)$.

We then insert the $\mathbf{E}$ and $\mathbf{B}$ from equations (2.43) into (2.42) and simplify the result. See the appendix, section A.2.

$$H = \frac{1}{2}\Big(\big(\partial_t q\big)^2 + \omega_n^2 q^2(t)\Big) \tag{2.45}$$

From a classical physics perspective, we can think of $q(t)$ as a generalised kind of coordinate that, according to equation (2.43), describes the time-dependent amplitude of the magnetic field. The time derivative, $\partial_t q$, then corresponds to a generalised momentum that, again according to equation (2.43), gives the time-dependent electric field amplitude. Since both the kinetic and potential terms in equation (2.45) are squared, the amplitudes of both fields would (as expected) display a harmonic oscillation.

We are now ready to quantise the generalised coordinate q, according to the strategy discussed in section 2.2. We promote each value $\{q \in \mathbb{R}\}$ to a state of the system, $\{|q\rangle\}$, and an operator $\hat{q}$ will give the numbers back when operating on these states.

$$\hat{q}\,|q\rangle = q\,|q\rangle \qquad \text{with} \qquad q \in \mathbb{R} \tag{2.46}$$

As discussed before (section 2.2), this move introduces superpositions and an abstract Hilbert space.

The classical generalised momentum, $\partial_t q$, is also replaced by the corresponding quantum mechanical operator, $\hat{p}$. These operators are the ones from equations (2.28). We summarise the quantisation procedure (in the basis $\{|q\rangle\}$).

$$\begin{cases} q(t) \to \hat{q} & \text{(2.47a)} \\ \partial_t q \ \to \hat{p} = -\mathrm{i}\hbar\hat{\partial}_q & \text{(2.47b)} \end{cases}$$

Inserting this into equation (2.45) we get our quantum mechanical Hamiltonian.

$$H = -\frac{\hbar^2}{2}\,\hat{\partial}_q^2 + \frac{\omega_n^2}{2}\,\hat{q}^2 \tag{2.48}$$

Given this Hamiltonian, we can solve the time-independent Schrödinger equation in the position basis $\{|q\rangle\}$ to get a set of eigenfunctions, $\psi_n(q) := \langle q|n\rangle$, and their eigenenergies. Here we simply summarise the solution of this well know quantum harmonic oscillator problem [61] in figure 2.2.

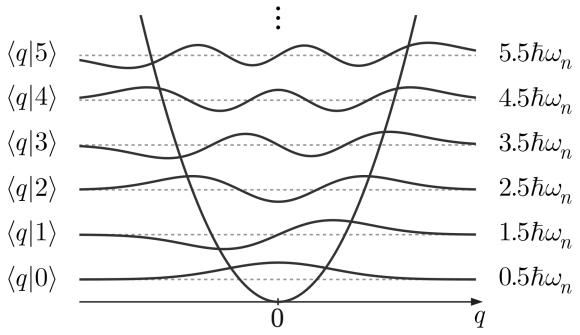

Figure 2.2: The coordinate q corresponds to the field amplitude of a single mode in an optical cavity. The potential energy function is a harmonic potential. Eigenstate wavefunctions are plotted at their respective energy (dashed lines). These states, $\{|n\rangle : n \in \mathbb{N}_0\}$, constitute the Fock basis for the electromagnetic cavity.

Thus what we have found is a discretisation of the energy spectrum for the electromagnetic field, where each energy level has a particular superposition of field amplitudes. Since all states are equidistant we can identify them as states corresponding to particles of light, or photons. These states form an alternative basis, $\{|n\rangle\}$ with $n \in \mathbb{N}_0$, for our Hilbert space—the so-called Fock basis.

We then define two *ladder operators*: $\hat{a}^\dagger$ to create a photon, going up the energy ladder, and $\hat{a}$ to destroy photons, going down the ladder.

$$\hat{a}^\dagger |n\rangle = \sqrt{n+1}\ |n+1\rangle \qquad ; \qquad \hat{a}\,|n\rangle = \sqrt{n}\ |n-1\rangle \tag{2.49}$$

The derivation of these operators will show how they relate to $\hat{q}$ and $\hat{p}$ [60, 62].

$$\hat{q} = \sqrt{\frac{\hbar}{2\omega_n}}(\hat{a}^\dagger + \hat{a}) \qquad \text{and} \qquad \hat{p} = \mathrm{i}\sqrt{\frac{\hbar\omega_n}{2}}(\hat{a}^\dagger - \hat{a}) \tag{2.50}$$

With this, we rewrite equation (2.48) in terms of $\hat{a}$ and $\hat{a}^\dagger$.

$$\hat{H} = \hbar\omega_n \left(\hat{a}^\dagger\hat{a} + \frac{\hat{\mathbb{1}}}{2}\right) \tag{2.51}$$

As a final simplification, we can redefine what we consider zero energy, thus removing the $\hat{\mathbb{1}}/2$ term and expressing the cavity Hamiltonian only in terms of the number operator, $\hat{N} = \hat{a}^\dagger\hat{a}$.

$$\hat{H} = \hbar\omega_n\, \hat{a}^\dagger\hat{a} \tag{2.52}$$

Having carried out a quantisation of the field, we can construct an electric field operator, $\hat{\mathbf{E}}$, by inserting equation (2.50) into the electric field from equation (2.43) [60].

$$\mathbf{E}_n^{\perp}(z) = \mathrm{i}\,\mathbf{e}_x \sqrt{\frac{\hbar\omega_n}{\epsilon_0 V}} \left(\hat{a}^{\dagger} - \hat{a}\right) \sin(k_n z) \tag{2.53}$$

Inserting this into the, previously semi-classical, minimal coupling Hamiltonian, equation (2.37), will produce a fully quantum mechanical theory.

The symbol $\mathcal{E}_\mathrm{c}$ is often used in the literature for the amplitude constant in equation (2.53). It is however typically derived, not for a standing wave, but for free field running-wave solutions, in which case the constant picks up a factor of $1/\sqrt{2}$ [63].

$$\mathcal{E}_\mathrm{c} := \sqrt{\frac{\hbar\omega_n}{2\epsilon_0 V}} \tag{2.54}$$

$\mathcal{E}_\mathrm{c}$ is referred to as the "vacuum electric field strength" [2], the "rms zero-point electric field" [64], or simply described as "the electric field strength associated with a single photon" [17]. In terms of this definition, we have a final form of the electric field operator.

$$\hat{\mathbf{E}}_n(z) = \mathrm{i}\,\mathbf{e}_x \sqrt{2}\,\mathcal{E}_\mathrm{c}\left(\hat{a}^{\dagger} - \hat{a}\right) \sin(k_n z) \tag{2.55}$$

2.6 Remarks on magnetic interactions

The equations we use for the polaritonic chemistry systems do not include magnetic interactions. Here we briefly motivate why we can omit them, and where in the derivations these terms got dropped.

For electromagnetic radiation, where the two fields are intertwined, we have that $|\mathbf{B}| = |\mathbf{E}|/c$ [59]. To estimate each field's interaction with a charged particle, we insert this into the Lorentz force, equation (2.2). This gives that magnetic forces are suppressed by a factor v/c compared to forces from electric fields. In the systems that we study, v/c is a small number (where typical velocities can be obtained from a momentum expectation value). Thus we can neglect effects from the magnetic fields.

Nevertheless, if we wanted to include magnetic interactions, they were stealthily omitted at two points in the preceding discussion. To include the interaction with the intrinsic magnetic moment of particles, also known as *spin*, we start with the relativistic Dirac equation.

$$\mathrm{i}\hbar\gamma^{\mu}\partial_{\mu}\psi - mc\psi = 0 \tag{2.56}$$

Via a series of arguments, the non-relativistic *Pauli equation* can be derived from the Dirac equation [59]. Its Hamiltonian has a separate term, $q\hbar\hat{\boldsymbol{\sigma}}\cdot\mathbf{B}$, for spin–field interactions.

$$\hat{H} = \frac{1}{2m}\big(\hat{\mathbf{p}} - q\mathbf{A}\big)^2 + q\Phi + q\hbar\hat{\boldsymbol{\sigma}}\cdot\mathbf{B} \tag{2.57}$$

This term was not present in the minimal coupling Hamiltonian, equation (2.30), and these interactions were thus neglected from the start.

We should also clarify where the magnetic interactions due to orbital angular momentum were omitted. Equation (2.17c) tells us that the $\mathbf{B}$ field comes from the spatial derivatives of $\mathbf{A}$. However, when introducing the long-wavelength limit, in section 2.1.5, we removed the spatial variations in $\mathbf{A}$. Thus, in the long-wavelength limit, there are no external magnetic fields for particle velocities, also known as orbital angular momentum, to intact with.

2.7 Computational quantum chemistry

When it is energetically favourable atoms come together to form molecules, sharing the electrons in a configuration that breaks the spherical symmetry of a solitary atom. To take the general case, we have N_n nuclei with positive charges, and N_e electrons, each with a single negative elementary charge. In this section, we will discuss how such a system is described within quantum chemistry.

To get a feeling for why these problems are hard, we can span the Hilbert space for the $N_\mathrm{n} + N_\mathrm{e}$ particles in the position basis. Each particle brings three spatial degrees of freedom. For the positions of the nuclei we use the vectors $\{\mathbf{R}_n\}$ where $n \in \{1, \cdots, N_\mathrm{n}\}$, and for the positions of the electrons use the vectors, $\{\mathbf{r}_e\}$ where $e \in \{1, \cdots, N_\mathrm{e}\}$. With Cartesian coordinates the uncountably infinite set of position eigenstates are $|\mathbf{R}_n\rangle := |X_n, Y_n, Z_n\rangle$ for nuclei, and $|\mathbf{r}_e\rangle := |x_e, y_e, z_e\rangle$ for electrons (here, using a condensed notation for the tensor product, $|a, b\rangle := |a\rangle \otimes |b\rangle$). With this, we can span the full Hilbert space.

$$\Big\{\, |\mathbf{R}_1, \cdots, \mathbf{R}_{N_\mathrm{n}}, \mathbf{r}_1, \cdots, \mathbf{r}_{N_\mathrm{e}}\rangle : \forall \text{ combinations} \Big\} \tag{2.58}$$

A core problem is the sheer size of this basis, in conjunction with admitting any superposition of states. For most physical systems, this is going to make any flexible construction for state descriptions too large to handle numerically. And unfortunately, there are no known analytic solutions to these quantum many-body problems. To then consider the time-evolution of states adds additional complexity. The solution is to apply some reasonable approximative methods:

A ubiquitous strategy for molecular systems is to separate electronic and nuclear degrees of freedom, to then treat the electronic problem first and the nuclear second. This is done with the so-called Born–Oppenheimer approximation (section 2.7.1). There are many numerical techniques that use this approximation, where each method has its blend of benefits and drawbacks, with different accuracies and demands on computational resources.

The Hartree-Fock method (section 2.7.3) is a foundational method. But there are various extensions of this method. The ones that are discussed in this thesis are all based on the ideas of *configuration interaction* (section 2.7.4), and they are MCSCF (section 2.7.5) and CASSCF (section 2.7.6). In these discussions, we consider a non-relativistic Hamiltonian in the Coulomb Gauge (section 2.1.4), internal complexities of the nuclei are overlooked, and so are the magnetic interactions between charged particles, which have spin and orbital angular momentum.

2.7.1 The Born–Oppenheimer approximation and the molecular Hamiltonian

Due to the vast Hilbert space, direct numerical representations of the basis in equation (2.58) quickly become computationally intractable. Nevertheless, for a given Hamiltonian there exists some set of stationary eigenstates. We can imagine having found such a state, $|\Psi\rangle$. As a toy representation, let one axis be labelled "$\mathbf{R}$" and it represents all nuclear degrees of freedom, and for the electronic degrees of freedom we use a second axis labelled "$\mathbf{r}$". Since the theory builds on complex numbers, we might require both real and imaginary components, but for illustrative clarity, we imagine a single-component eigenstate wavefunction $\langle \mathbf{R}, \mathbf{r}|\Psi\rangle = \Psi(\mathbf{R}, \mathbf{r})$. See figure 2.3.

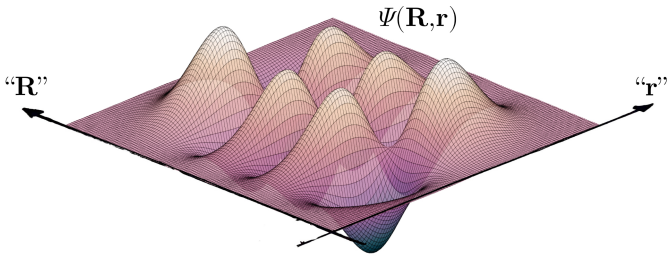

Figure 2.3: Schematic representation of a wavefunction for a molecule. The axis "$\mathbf{R}$" represents all degrees of freedom for the nuclei. The axis "$\mathbf{r}$" represents all degrees of freedom for the electrons. The function $\Psi(\mathbf{R}, \mathbf{r})$ is meant to illustrate an eigenfunction on this space for the molecular Hamiltonian.

Note that while this argument applies to only a single eigenstate, it can be extended to calculations involving multiple excited states.

Instead of solving for the entire wavefunction, represented in figure 2.3, in the Born–Oppenheimer approximation, we select some number of position eigenstates for the nuclei $\{|\mathbf{R}^i\rangle\}$, and then solve for the wavefunction of the electronic degrees of freedom once for each of the chosen nuclear position eigenstates. I.e. instead of the function $\Psi(\mathbf{R}, \mathbf{r})$, from figure 2.3, we calculate a family of functions, $\{\phi_{\mathbf{R}^i}(\mathbf{r})\}$, as illustrated in figure 2.4.

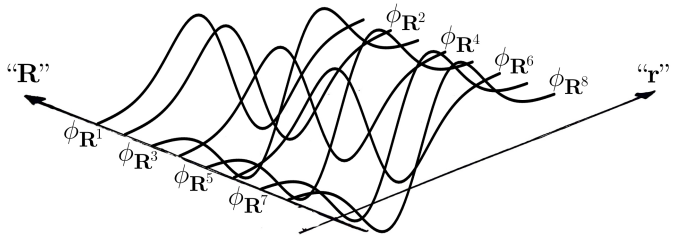

Figure 2.4: A separation of the degrees of freedom, according to the Born–Oppenheimer approximation, is applied to the function in figure 2.3. The axis “$\mathbf{R}$” represents all degrees of freedom for the nuclei. The axis “$\mathbf{r}$” represents all degrees of freedom for the electrons. The curves, $\{\phi_{\mathbf{R}^i}(\mathbf{r})\}$, represent wavefunctions for the electronic degrees of freedom “$\mathbf{r}$”.

To solve for an electronic eigenfunction $\phi_{\mathbf{R}^i}(\mathbf{r})$ independently, we need to derive the so-called electronic Hamiltonian, $\hat{H}_\mathrm{e}$, from a Hamiltonian for the full system. See the appendix, section A.3. In the derivation, two approximations are introduced. Together they are known as the *adiabatic approximation*, and they neglect the derivative along $\mathbf{R}$, which is induced by changes between neighbouring electronic solutions.

$$\begin{cases} \hat{\boldsymbol{\nabla}}_\mathbf{R}\, \phi_\mathbf{R}(\mathbf{r}) := \mathbf{0} & \text{(2.59a)} \\ \hat{\nabla}^2_\mathbf{R}\, \phi_\mathbf{R}(\mathbf{r}) := 0 & \text{(2.59b)} \end{cases}$$

This decouples the electronic degrees of freedom from the nuclear ones and effectively says that we can determine electronic eigenstates without knowing the nuclear wavefunction. (Their details are discussed in the derivation of $\hat{H}_\mathrm{e}$, in section A.3 of the appendix.) In this approximation, the full Hamiltonian can then be written as a sum of the nuclear kinetic energy, $\hat{T}_\mathrm{n}$ and the electronic Hamiltonian $\hat{H}_\mathrm{e}^{\mathbf{R}^i}$.

$$\hat{H} = \hat{T}_\mathrm{n} + \hat{H}_\mathrm{e}^{\mathbf{R}^i} \tag{2.60}$$

The electronic Hamiltonian takes the position of the nuclei, $\mathbf{R}^i$, as a given parameter, and it contains four terms.

$$\hat{H}_{\mathrm{e}}^{\mathbf{R}^i} = \hat{T}_{\mathrm{e}} + \hat{V}_{\mathrm{ne}}^{\mathbf{R}^i} + \hat{V}_{\mathrm{nn}}^{\mathbf{R}^i} + \hat{V}_{\mathrm{ee}} \tag{2.61}$$

$$\begin{aligned} \hat{T}_{\mathrm{e}} &= -\sum_e \frac{1}{2}\hat{\nabla}_{\mathbf{r}_e}^2 \qquad ; \qquad \hat{V}_{\mathrm{ne}}^{\mathbf{R}^i} = \sum_n \sum_e \frac{Z_n}{\left|\hat{\mathbf{R}}_n^i - \hat{\mathbf{r}}_e\right|} \\ \hat{V}_{\mathrm{nn}}^{\mathbf{R}^i} &= \sum_n \sum_{\nu>n} \frac{Z_n Z_\nu}{\left|\hat{\mathbf{R}}_n^i - \hat{\mathbf{R}}_\nu^i\right|} \qquad ; \qquad \hat{V}_{\mathrm{ee}} = \sum_e \sum_{\epsilon>e} \frac{1}{\left|\hat{\mathbf{r}}_e - \hat{\mathbf{r}}_\epsilon\right|} \end{aligned} \tag{2.62}$$

Here, $\hat{T}_{\mathrm{e}}$ is the kinetic energy for the electronic degrees of freedom. With the nuclei clamped at the position eigenstates $\{|\mathbf{R}^i\rangle\}$, $\hat{V}_{\mathrm{ne}}^{\mathbf{R}^i}$ is the potential energy for the electronic degrees of freedom due to the nuclei, and $\hat{V}_{\mathrm{nn}}^{\mathbf{R}^i}$ is the potential energy between the clamped nuclei. Finally, $\hat{V}_{\mathrm{ee}}$ is the potential energy for the electronic degrees of freedom due to electron–electron repulsions.

The problem of solving for the electronic wavefunction, $\phi_{\mathbf{R}^i}(\mathbf{r})$, is then handled with numerical methods (such as the ones discussed in sections 2.7.3 – 2.7.6), which are implemented in program packages such as Molpro, Molcas, or Gaussian, to name a few. For any particular nuclear state $|\mathbf{R}^i\rangle$, at least the lowest eigenvalue for the ground-state is calculated. But for the studies in this thesis, multiple eigenvalues, $\{E_j\}$, are needed to describe the dynamics of excited electronic states. Thus, the following electronic eigenvalue equation is solved for a couple of eigenvalues, still independently for each $|\mathbf{R}^i\rangle$.

$$\hat{H}_{\mathrm{e}}^{\mathbf{R}^i}\, \phi_{\mathbf{R}^i,\, j}(\mathbf{r}) = E_j(\mathbf{R}^i)\, \phi_{\mathbf{R}^i,\, j}(\mathbf{r}) \tag{2.63}$$

This calculation can be run in parallel for as many clamped nuclear configurations as needed, and energy eigenvalues are associated with each other between neighbouring configurations, creating *potential energy surfaces*, $E_j(\mathbf{R}^i)$, as functions of nuclear positions (further discussed in section 2.7.2).

Since the electronic wavefunctions $\{\phi_{\mathbf{R}^i}(\mathbf{r})\}$ are solved for independently at each configuration of position eigenstates of the nuclei, $\{|\mathbf{R}_i\rangle\}$, these wavefunctions are normalised to unity. With sufficiently closely spaced points in $\{\mathbf{R}^i\}$, we could in principle recreate the full wavefunction $\Psi(\mathbf{R}, \mathbf{r})$ (from figure 2.3) by multiplying each $\{\phi_{\mathbf{R}^i}(\mathbf{r})\}$ (from figure 2.4) by the appropriate complex factors.[4] We call these factors $\{\psi(\mathbf{R}^i)\}$, and taken together they constitute a wavefunction $\psi(\mathbf{R}) := \{\psi(\mathbf{R}^i)\}$, known as a nuclear wavefunction. With the electronic potential energy surfaces, eigenstates for this nuclear wavefunction

[4] Note that there is one caveat with reconstructing $\Psi(\mathbf{R}, \mathbf{r})$ (figure 2.3) from $\{\phi_{\mathbf{R}^i}(\mathbf{r})\}$ (figure 2.4): The full wavefunction $\Psi(\mathbf{R}, \mathbf{r})$ was assumed to be an eigenfunction to the full molecular Hamiltonian, while the family of functions $\{\phi_{\mathbf{R}^i}(\mathbf{r})\}$ is obtained after the adiabatic approximation in equation (2.59). Thus we need the terms in the adiabatic approximation to be small to get an accurate reconstruction.

can be determined, and time-evolution can be carried out. This is, of course, all done under the crucial assumption of the Born–Oppenheimer approximation; that the electronic wavefunctions can be calculated without specifying the nuclear wavefunction.

As a final remark, numerical implementations will reduce the number of spatial degrees of freedom by six (of five for diatomic molecules) by using relative coordinates for the clamped nuclei, and not absolute ones.

2.7.2 Potential energy surfaces for the diatomic MgH^+

Since all papers in this thesis [1–3] concern diatomic molecules (MgH^+ and CO), this section will examine potential energy surfaces through the lens of such comparatively simple molecules.

For diatomic molecules, the nuclear degrees of freedom can be modelled by considering only the relative distance between the nuclei. In this picture rotations and translations are absent. Remember that the Born–Oppenheimer approximation stipulates solving for the electronic wavefunctions with position eigenstates of the nuclei, thus there are no rotations or translations at this stage. Under the central assumption that the coupling between nuclear and electronic degrees of freedom is negligible, we can introduce rotations and translations in the subsequent nuclear wavefunction. However, they are still commonly omitted, since, in many situations, energies associated with rotations and translation are smaller than those for vibrations and electronic excitations (which we study here). All papers in this thesis [1–3] rely on an assumption similar to this, and we omit molecular rotations and translations.

The separation between the two nuclei is thus the single remaining nuclear degree of freedom, and we label it with R. The chosen set of nuclear eigenstates can then be interpreted as gridpoints along R, and potential energy surfaces, $E_j(R)$, are calculated along this coordinate. An example of this is shown in figure 2.5.

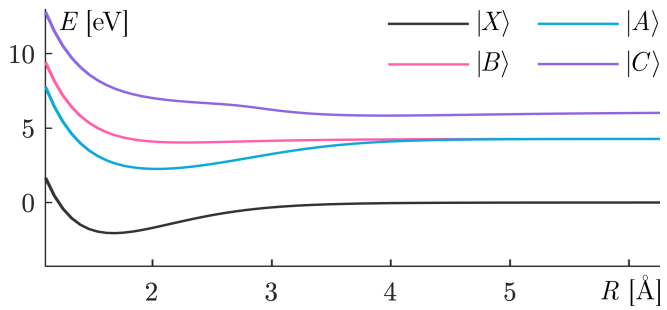

Figure 2.5: The four lowest potential energy surfaces of the diatomic MgH^+ molecule, as functions of the nuclear separation, R.

It is under the influence of these potential energies that the nuclear wavefunction $\psi(R)$ can be time-evolved, which then models the electronic and vibrational state of the molecule, and can indicate molecular dissociation if wave packets reach large values of R.

2.7.3 Hartree–Fock theory

Even for a simple molecule such as the diatomic MgH^+, the spatial degrees of freedom associated with the 12 electrons will make it infeasible to solve for eigenstates of the electronic Schrödinger equation using the states in the position basis.[5] Fortunately, the Hartree–Fock method [65] allows us to describe the rough features of the electronic ground-state, with a relatively small number of *molecular orbitals* (described below), and the method is possible to extend to more exact solutions with a manageable scaling in computational cost (sections 2.7.4 – 2.7.6).

The method determines a set of mutually orthonormal functions, that are more or less spatially concentrated around the clamped nuclei. These are so-called molecular orbitals, $\{\phi_i(\mathbf{r})\}$, where $\mathbf{r}$ is a regular position vector in three dimensions. To construct these functions, we start with a set of basis-functions that are similar to the known solutions for the hydrogen atom. The motivation for this is that the electron density around each nucleus is assumed to share features with the electron densities around single atoms. While these basis-functions will not be orthogonal when compared between nuclei, they will be linearly independent, and from K basis-functions one can still form K orthonormal orbitals. The orbitals are then used to construct an electronic wavefunction.

However, we must respect the antisymmetry condition of fermionic wavefunctions; where exchanging both position and spin associated with any two particles will introduce a global phase of -1, but otherwise leave the state unaffected. This implies that any orbital can only be used twice in constructing the total wavefunction, once as a spin-up orbital, and once with spin-down.[6] Orbitals that include the spin degree of freedom are called spin-orbitals and we denote them $\{\varphi_i(\mathbf{x}_k)\}$ (where $\mathbf{x}_k$ is both a regular position vector in three dimensions as well as the spin label for the kth particle).

With these orbitals, a wavefunction in Hartree–Fock theory $\Phi_{\mathrm{HF}}(\mathbf{x})$ is constructed from an antisymmetric linear combination. The pattern for creating this antisymmetric linear combination maps onto the pattern of calculating determinants, hence we use the determinant notation to express what would

[5] A naive calculation using only 12 grid points for each of the 12 electrons yields a memory requirement on the order of terabytes.

[6] Since terms with magnetic forces (such as the spin-orbit coupling) are neglected in the employed Hamiltonian (see equation (A.30) in the appendix section A.3), there is no need to identify the spatial direction in which the spins are up or down.

otherwise be an unwieldy sum with $N_\mathrm{e}!$ terms.

$$\Phi_\mathrm{HF}(\mathbf{x}) = \frac{1}{\sqrt{N_\mathrm{e}!}} \begin{vmatrix} \varphi_1(\mathbf{x}_1) & \cdots & \varphi_N(\mathbf{x}_1) \\ \vdots & \ddots & \vdots \\ \varphi_1(\mathbf{x}_N) & \cdots & \varphi_N(\mathbf{x}_N) \end{vmatrix} \tag{2.64}$$

This wavefunction is called a Slater determinant [65].

Without going over all details for how to determine the ground-state Slater determinant for the given basis set, we will sketch the challenge and a solution: The biggest challenge comes from the electron–electron interaction term, $\hat{V}_\mathrm{ee}$, in equation (2.62). Due to this term, calculating the energy associated with some electronic degree of freedom depends on knowing the wavefunction for all other degrees of freedom. The solution is to use the calculus of variations and Lagrange multipliers to determine a stationary point, under the constraint that the orbitals remain orthogonal.

$$\mathcal{L}\big[\{\phi_i\}\big] = \langle \Phi_\mathrm{HF} | \hat{H} | \Phi_\mathrm{HF} \rangle + \sum_{i,j} \lambda_{ij} \big(\delta_{ij} - \langle \phi_i | \phi_j \rangle \big) \tag{2.65}$$

At a stationary point, where the condition is that $\delta\mathcal{L} = 0$, the variational principle guarantees that the wavefunction that we find has the lowest possible energy that the method can produce [65]. For numerical implementation, the so-called Roothaan equation can be derived (not shown here, see Jensen [65]) from equation (2.65).

$$FC = SC\varepsilon \tag{2.66}$$

In short, F is the so-called Fock matrix of energies from the Hamiltonian, expressed in the chosen basis-functions, and F depends on the matrix C. It contains the coefficients that determine the superpositions of basis-functions that form the orbitals and then the Slater determinant—this is what we solve for. S is a matrix containing the overlap elements (inner products) between all the basis-functions. Finally, ε is a diagonal matrix of energies for each orbital. To solve the Roothaan equation (2.66) one starts from an initial guess, $C^{(0)}$, which allows us to calculate $F^{(0)}$. With $F^{(0)}$ we can then calculate a new matrix $C^{(1)}$, giving us $F^{(1)}$, and so on. Iterating this procedure allows us to take $C^{(N)}$ to the stationary point (within some predefined error tolerance). By the variational principle, the resulting state, $|\Phi_\mathrm{HF}\rangle$, has the lowest possible energy (that this method can produce), and it is thus identified as the ground-state of the system. This state is not a *true* ground-state however, since the energy is constrained by the chosen basis set, which does not span the entire Hilbert space, and it is calculated under the approximations previously discussed. Additionally, as we shall see in the coming sections (2.7.4 – 2.7.6), using a single Slater determinant limits what wavefunctions we can express.

2.7.4 Configuration interaction, CI

The Slater determinant allows us to optimise a wavefunction on a large number of degrees of freedom without too much numerical effort; what we need to store in memory is the coefficients that take the basis-functions to the molecular orbitals, $\{\varphi_i(\mathbf{x}_k)\}$. Unfortunately, the Slater determinant is unable to describe arbitrary wavefunctions. To examine this shortcoming, we will first consider particles without spin that are also distinguishable (without the anti-symmetry condition).

One way to construct a wavefunction for many degrees of freedom is to substitute the product of wavefunctions for each degree of freedom:

$$\Psi(\mathbf{r}_1, \mathbf{r}_2, \cdots, \mathbf{r}_N) \;\rightarrow\; \psi_1(\mathbf{r}_1)\psi_2(\mathbf{r}_1)\cdots\psi_N(\mathbf{r}_N) \tag{2.67}$$

This product wavefunction, also known as a Hartree product, will not be able to represent arbitrary wavefunctions. In particular, any wavefunction with entanglement between any of the degrees of freedom, $\{\mathbf{r}_1, \cdots, \mathbf{r}_N\}$, is not described by this construction. Thus, the Hartree product only describes the subset of *separable* wavefunctions. The Slater determinant in equation (2.64) is then a particular anti-symmetric superposition of such Hartree products. This superposition introduces entanglement, but the fundamental restriction that comes with a Hartree product remains; the Slater determinant is still restricted to only a subset of wavefunctions.

We can however improve on the space of functions that we can reach for some given basis set. If the basis contains K basis-functions, the construction is such that K is larger than the number of *occupied orbitals*, $N_\mathrm{e}/2$, that are needed to create the Slater determinant wavefunction. Therefore, it is possible to span a larger region of the (infinite) Hilbert space by incorporating some of the otherwise unoccupied $K - N_\mathrm{e}/2$ orbitals. This is achieved by constructing so-called *excited determinants*, where one or more of the occupied orbitals from a Harty-Fock Slater determinant, Φ_HF, is swapped for unoccupied ones. Swapping a single orbital results in a *singly excited* determinant, Φ_S, swapping two makes a *doubly excited* determinant, Φ_D, and so on. Note that these *excited determinants* will create a set of orthogonal wavefunctions (since all K orbitals are orthogonal to begin with), thus superpositions of these will span a larger subspace of our infinite Hilbert space.

$$\Phi_\mathrm{CI} = C\,\Phi_\mathrm{HF} + \sum_S C_S\,\Phi_S + \sum_D C_D\,\Phi_D + \cdots + \sum_X C_X\,\Phi_X \tag{2.68}$$

This means that a superposition of these orthogonal Slater determinants can get closer to the true ground-state, and achieve lower energy after the variational principle is applied. In the limit of a complete set of basis-functions, and for an infinite sum of these excited Slater determinants, the solution will be exact (of course still under the non-relativistic approximation, etc.).

In a configuration interaction calculation, the orbitals are first optimised in a standard Hartree–Fock calculation and then held fixed in all subsequent calculations. After determining how many excited determinants to include, we use the variational principle again to find a stationary point under the constraint that our configuration interaction wavefunction, Φ_{CI}, remains normalised.

$$\mathcal{L}\big[\Phi_{\mathrm{CI}}\big] = \langle \Phi_{\mathrm{CI}} | \hat{H} | \Phi_{\mathrm{CI}} \rangle + \lambda\big(1 - \langle \Phi_{\mathrm{CI}} | \Phi_{\mathrm{CI}} \rangle\big) \tag{2.69}$$

Under the $\delta\mathcal{L} = 0$ condition, one derives a large, so-called, CI matrix with energies on the diagonal, and some blocks with non-zero off-diagonal elements. Diagonalising this CI matrix gives us corrections that lower the ground-state energy. The higher-lying energies in this matrix now correspond to electronically excited states, and this calculation, as well as the two following methods in sections 2.7.5 and 2.7.6, can be used to create multiple potential energy surfaces such as those shown in figure 2.5 (section 2.7.2).

2.7.5 Multi-configurational self-consistent field, MCSCF

In contrast to configuration interaction, Multi-Configurational Self-Consistent Field, or MCSCF, does not hold the orbitals fixed when determining the coefficients for different determinants. Instead, the orbitals and superposition of exited determinants are optimised together in a single iterative algorithm. This increases the computational complexity for each iteration, and typically one will select fewer excited determinants compared to a configuration interaction calculation. When constrained to fewer excited determinants it will be more important to choose them wisely. One of the most popular schemes is called Complete Active Space Self-Consistent Field (CASSCF) [65], which is the method used in Papers I and II [1, 2], and discussed in section 2.7.6.

2.7.6 Complete active space self-consistent field, CASSCF

The idea behind CASSCF is that orbitals with higher energies will contribute less to the final electronic wavefunction, or in other words, that any coupling elements in the CI matrix will be small compared to the energy difference. Thus, in this method, spin orbitals are ordered by energy and a predetermined number of occupied and unoccupied orbitals from the energy ordering are selected to be part of the active space. See figure 2.6. Within the active space, all possible exited Slater determinants (distinguishing spin-up and spin-down orbitals) are included in an MCSCF calculation.

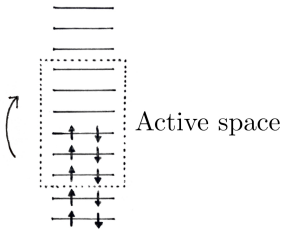

Figure 2.6: A number of occupied and unoccupied orbitals are selected for the active space of a CASSCF calculation. All permutations of exited Slater determinants in this space are included.

Selecting the appropriate orbitals to include in the active space is a challenge that can be made simpler by investigating the spatial distribution of the available orbitals. For instance, when describing bond breaking with large nuclear distances it will be important to include anti-bonding orbitals in the active space.

2.8 The Jaynes–Cummings model

In the early introduction of the Jaynes–Cummings model [11], the cavity mode is modelled by quantising the electromagnetic field in a procedure like the one in section 2.5, giving the Hamiltonian from equation (2.52).

$$\hat{H}_{\mathrm{c}} = \hbar\omega_n \, \hat{a}^\dagger \hat{a} \tag{2.70}$$

The ladder operators for the cavity field, $\hat{a}^\dagger$ and $\hat{a}$, are simple in the Fock basis, $\{|n\rangle\}$ (discussed in relation to figure 2.2), and this will be our choice of basis for the cavity moving forward. It is also used in the calculations for all papers in this thesis [1–3].

In the Jaynes–Cummings model, the emitter was a two-level system (also known as a qubit) which is commonly associated with atoms but can also describe, for instance, two vibrational levels in a molecule. Though modern studies of polaritonic chemistry often consider physical phenomena that require more detailed models of emitters, we shall here introduce the Jaynes–Cummings model for an atom, and in section, 2.9.1, we consider a richer model with a molecule as an extension of the following discussion.

The two-level system is modelled with a two-dimensional Hilbert space, here spanned by the energy eigenstates $\{|g\rangle, |e\rangle\}$. The state $|g\rangle$ is a ground-state that we here take to have energy 0, and $|e\rangle$ is an excited state with energy E_{a}. The projection operator $|e\rangle\langle e|$ is often expressed in terms of the excitation operator, $\hat{\sigma}^\dagger = |e\rangle\langle g|$, and the de-excitation operator, $\hat{\sigma} = |g\rangle\langle e|$, i.e. $\hat{\sigma}^\dagger\hat{\sigma} = |e\rangle\langle e|$, and we can form a Hamiltonian for the atom.

$$\hat{H}_{\mathrm{a}} = E_{\mathrm{a}} \, \hat{\sigma}^\dagger \hat{\sigma} \tag{2.71}$$

In section 2.3 we derived an interaction term between a charged particle and the field, under the Coulomb gauge (section 2.1.4). We further established that with multiple particles, the multiple interaction terms can be approximated as one interaction with a total dipole $\hat{\mathbf{d}}$, using the dipole approximation discussed in section 2.4.

$$\hat{H}_{\mathrm{int}} = -\hat{\mathbf{d}} \cdot \hat{\mathbf{E}}(t) \qquad \text{where} \qquad \hat{\mathbf{d}} := \sum_{n=1}^{N} q_n \hat{\mathbf{r}}_n \tag{2.72}$$

When compared to equation (2.40), $\hat{\mathbf{E}}$ has now been promoted to an operator according to equation (2.55), from the second quantisation procedure in section 2.5.

When considering an atom, spherical symmetry implies that the dipole operator will be the same in any direction. Thus, without loss of generality, we consider the field polarization and dipole operator in the same direction and let that direction be $\mathbf{e}_x$.

In equation (2.72) we see that $\hat{\mathbf{d}}$ is a diagonal operator in the position basis.

However, given a complete set of electronic eigenstates $\{|\Phi_1\rangle, |\Phi_2\rangle, \cdots\}$ (on the electronic degrees of freedom) we can re-express the dipole operator in that basis.

$$\hat{\mathbf{d}} = \mathbf{e}_x \sum_{e,i,j} q_e \, |\Phi_i\rangle \, \langle\Phi_i|\hat{x}_e|\Phi_j\rangle \, \langle\Phi_j| \tag{2.73}$$

In the Jaynes–Cummings model only two electronic states are considered, thus $i, j \in \{1, 2\}$. Note that the contribution from the nucleus is zero when the atom is centred at the origin, and also the diagonal terms will vanish since $\hat{x}_e$ is an odd function.

$$\hat{\mathbf{d}} = \mathbf{e}_x \sum_{e} q_e \, |\Phi_2\rangle \, \langle\Phi_2|\hat{x}_e|\Phi_1\rangle \, \langle\Phi_1| + q_e \, |\Phi_1\rangle \, \langle\Phi_1|\hat{x}_e|\Phi_2\rangle \, \langle\Phi_2| \tag{2.74}$$

We define these off-diagonal matrix elements (multiplied by the charge) as the *transition dipole moment,* $q_e\langle\Phi_2|\hat{x}_e|\Phi_1\rangle := \mu$, and it follows from definitions that $q_e\langle\Phi_1|\hat{x}_e|\Phi_2\rangle = \mu^*$.

$$\hat{\mathbf{d}} = \mathbf{e}_x \left(\mu \, |\Phi_2\rangle\langle\Phi_1| + \mu^* \, |\Phi_1\rangle\langle\Phi_2| \right) \tag{2.75}$$

The operator $|\Phi_2\rangle\langle\Phi_1|$ excites the electronic state, and $|\Phi_1\rangle\langle\Phi_2|$ de-excites it. However, it is not necessary for the final model to include all the details in the electronic degrees of freedom. Instead, we only want to keep track of the particular superposition of the electronic states. For this, we simplify the (truncated) basis $\{|\Phi_1\rangle, |\Phi_2\rangle\}$ into a two-dimensional Hilbert space spanned by states $\{|g\rangle, |e\rangle\}$, which were mentioned at the beginning of this section. This allows us to keep track of the electronic state populations and their relative phase. The transition operators from equation (2.75) can now be written in terms of simpler de-excitation and excitation operators, $\hat{\sigma} = |g\rangle\langle e|$ and $\hat{\sigma}^\dagger = |e\rangle\langle g|$.

$$\hat{\mathbf{d}} = \mathbf{e}_x \left(\mu \, \hat{\sigma}^\dagger + \mu^* \, \hat{\sigma} \right) \tag{2.76}$$

We then insert this result into equation (2.72), along with the electric field operator from equation (2.55).

$$\hat{H}_{\text{int}} = -\mathrm{i}\sqrt{2} \, \mathcal{E}_{\text{c}} \left(\mu \, \hat{\sigma}^\dagger + \mu^* \, \hat{\sigma} \right) \left(\hat{a}^\dagger - \hat{a} \right) \sin(k_n \, z) \tag{2.77}$$

Since the electronic eigenfunctions from equation (2.74) are only determined up to a phase we can choose μ to be purely imaginary and then re-express μ in terms of a real number, i.e. $\mu \to \mathrm{i}\mu$ and $\mu^* \to -\mathrm{i}\mu$ where $\mu \in \mathbb{R}$.

$$\hat{H}_{\text{int}} = \sqrt{2} \, \mathcal{E}_{\text{c}} \, \mu \left(\hat{\sigma}^\dagger - \hat{\sigma} \right) \left(\hat{a}^\dagger - \hat{a} \right) \sin(k_n \, z) \tag{2.78}$$

Note that we have a spatial dependence from the mode function (in our example, the z dependence in $\sin(k_n \, z)$). It is common to remove this by evaluating

the mode function at some particular region where emitters are assumed to be. Thus, assuming the atom is at the centre of the cavity, $\sin(k_i z) = 1$. We also group the other prefactors into $g := -\sqrt{2}\mu\,\mathcal{E}_\mathrm{c}$ and then expand the tensor product of the operators.

$$\hat{H}_\mathrm{int} = g\left(\hat{\sigma}^\dagger\hat{a} - \hat{\sigma}\hat{a}^\dagger - \hat{\sigma}^\dagger\hat{a}^\dagger + \hat{\sigma}\hat{a}\right) \tag{2.79}$$

We are about to simplify this expression further, but for that purpose, we need two things. First, from this point forward we will assume resonance, i.e. that the photon energy in the cavity mode matches (or at least is very close to) the energy of the atomic transition, $E_\mathrm{a} = \hbar\omega_n$.[7] Second, we specify a basis for the combined atom–cavity system. Since before, we have the basis $\{|g\rangle, |e\rangle\}$ for the atom, and the Fock basis $\{|n\rangle\}$ for the cavity. A product basis for the combined system is then formed from the two bases.

$$\left\{\, |g,n\rangle\,, |e,n\rangle \,:\, n \in \mathbb{N}_0 \right\} \tag{2.80}$$

Above, we use a condensed notation for the tensor product: $|\alpha,\beta\rangle := |\alpha\rangle\otimes|\beta\rangle$.

To simplify equation (2.79), notice that the term $\hat{\sigma}^\dagger\hat{a}^\dagger$ couples a state where the atom is in its ground-state and the cavity has n photons, to that of an excited atom and $n+1$ photons, i.e. $|g,n\rangle \to |e,n{+}1\rangle$. These states have a comparatively large energy difference. Similarly, the term $\hat{\sigma}\hat{a}$ couples the same states, but in the reverse direction. As long as the difference in energy between these states is much larger than the coupling strength, g, the mixing of these states will be small. Or put differently, the terms $\hat{\sigma}^\dagger\hat{a}^\dagger$ and $\hat{\sigma}\hat{a}$—known as the counter-rotating terms—are responsible for very little population transfer between the coupled states. Therefore, in the Jaynes–Cummings model, these counter-rotating terms are neglected and the interaction Hamiltonian is simplified.

$$\hat{H}_\mathrm{int} = g\left(\hat{\sigma}^\dagger\hat{a} + \hat{\sigma}\hat{a}^\dagger\right) \tag{2.81}$$

This simplification is called the rotating wave approximation.

Adding together the Hamiltonians in equations (2.70), (2.71), and (2.81) gives us the final Jaynes–Cummings Hamiltonian.

$$\hat{H} = \hbar\omega_n\,\hat{a}^\dagger\hat{a} + E_\mathrm{a}\,\hat{\sigma}^\dagger\hat{\sigma} + g\left(\hat{\sigma}^\dagger\hat{a} + \hat{\sigma}\hat{a}^\dagger\right) \tag{2.82}$$

Due to the off-diagonal elements from the interaction Hamiltonian, $g(\hat{\sigma}^\dagger\hat{a} + \hat{\sigma}\hat{a}^\dagger)$, the product basis from equation (2.80) is not the stationary eigenstates of the combined system. Still, under the resonance assumption, $E_\mathrm{a} = \hbar\omega_n$, we

[7] Most of the studies in polaritonic chemistry work with resonance; where the chemistry modifying effect is as strong as possible. This assumption typically rests on being able to tune the parameters of the cavity, and thus the photon energy $\hbar\omega_n$, to get the desired resonance.

diagonalise the Hamiltonian, with what is referred to as a polaron transformation [66], and the results turn out to be central to a lot of what we do in polaritonic chemistry. We will skip the computational details and summarise the results, see figure 2.7.

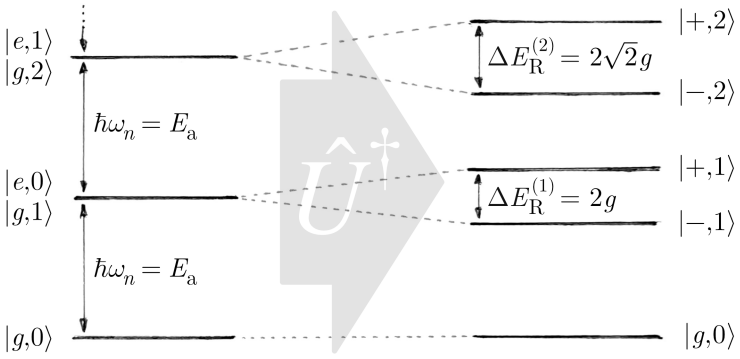

Figure 2.7: Rabi splitting, ΔE_R, in the energies after a unitary polaron diagonalization of Jaynes–Cummings Hamiltonian. With the resonance condition, $\hbar\omega_n = E_\mathrm{a}$, the left-hand side shows the degenerate energies of states in the initial product basis (of the emitter and cavity field). On the right-hand side, the diagonalisation of the Hamiltonian causes the energies in the resulting *polaritonic* eigenstates to split up [67]. Note how the Rabi splitting, ΔE_R, depends on the strength of the light–matter coupling, g.

The product states that are degenerate in energy, will form superpositions of excitation in the matter and cavity system which, depending on their relative phase, will either be lower in energy (the *lower polaritonic state*, such as $|-,1\rangle$) or higher in energy (the *upper polaritonic state*, such as $|+,1\rangle$). Assuming resonance, the polaritonic states are equal mixtures of the excited atom and the excited field [68].

$$\begin{aligned} |-,n\rangle &= \frac{1}{\sqrt{2}}\big(\,|e,n\text{-}1\rangle - |g,n\rangle\,\big) \\ |+,n\rangle &= \frac{1}{\sqrt{2}}\big(\,|e,n\text{-}1\rangle + |g,n\rangle\big) \end{aligned} \tag{2.83}$$

2.8.1 Rabi oscillations

If the system is initially in a product state, such as an initial excitation in the emitter, $|e, 0\rangle$, the excitation will oscillate sinusoidally without dampening, between the emitter and the cavity. This phenomenon is called Rabi oscillations, and the characteristic frequency, Ω_{R}, is the so-called Rabi frequency.

$$\Omega_{\mathrm{R}} = \frac{2g}{\hbar}\sqrt{N} \tag{2.84}$$

For completeness, we here include the dependence on the number of atoms, N, which in our discussion so far has been $N = 1$.

Note the physical interpretation of this oscillation. If an excitation is passed back and forth between the states $|g, 1\rangle$ and $|e, 0\rangle$, the atom is continuously emitting and absorbing the cavity photon, going from excited to ground-state, and then back again to start over.

2.9 Extensions of the Jaynes–Cummings model

For applications within polaritonic chemistry, the original Jaynes–Cummings model—as described by the Hamiltonian in equation (2.82)—is extended in some of the various ways discussed in the introduction (section 1.1). When considering studies in chemistry, the emitter often requires more detail than a basic two-level system. For instance, Paper III [3] uses a diatomic CO molecule, while Paper I and II [1, 2] uses a diatomic MgH^+. These emitters have to be modelled detailed enough to encompass vibrational and dissociative processes, and an internuclear distance is introduced (section 2.9.1). In Papers I and III [1, 3], along with the molecule, the model also incorporates an ensemble of two-level systems (section 2.9.2).

Since none of the papers in this thesis considers larger molecules, we will restrict the following discussion to diatomic molecules.

2.9.1 A molecular Jaynes–Cummings model

The tools and approximations from computational quantum chemistry (section 2.7) enable us to characterise the electronic and vibrational states of a diatomic molecule as nuclear wavefunctions evolving under the influence of one-dimensional potential energy surfaces [69, 70]. Here, each surface represents a particular electronic eigenstate, calculated under the Born-Oppenheimer approximation (here without corrections for the adiabatic approximation). As an example, let us consider two electronic states of some hypothetical diatomic molecule, in figure 2.8.

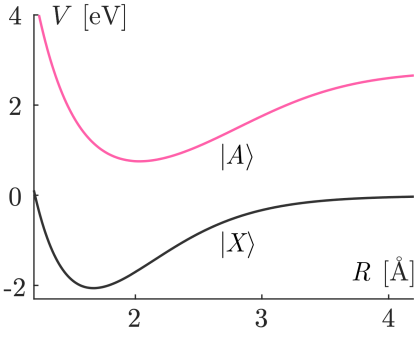

Figure 2.8: Potential energy surfaces of the electronic ground-state $|X\rangle$, and an excited state $|A\rangle$ for a hypothetical diatomic molecule. The coordinate R is the internuclear distance in a hypothetical diatomic molecule.

The Hamiltonian for the molecule–cavity system is very similar to the atomic case in equation (2.82), but we have to introduce a term for the kinetic energy of the nuclear motion, $-(1/2m)\,\partial_R^2$ (where m is the reduced mass for the system). We also have to accommodate that some values now are functions of R, such as the energies of both states, and the transition dipole moment $\mu(R)$, which makes the previously single-value coupling, g, a function of internuclear distance R.

$$\hat{H} = \hbar\omega_n \hat{a}^\dagger \hat{a} - \frac{1}{2m}\,\partial_R^2 + E_X(R)\,\hat{\sigma}\hat{\sigma}^\dagger + E_A(R)\,\hat{\sigma}^\dagger\hat{\sigma} + g(R)\left(\hat{\sigma}^\dagger\hat{a} + \hat{\sigma}\hat{a}^\dagger\right) \quad (2.85)$$

If the energy of the photon is identical to the energy difference between $|X\rangle$ and $|A\rangle$ at some point along R, we can say that the cavity is resonant to the electronic transition $|X\rangle \leftrightarrow |A\rangle$. For simplicity, we limit the consideration to the potential energy surface of the system ground-state, $|X, 0\rangle$, and no more than a single excitation in the system, i.e. we also include $|X, 1\rangle$ and $|A, 0\rangle$. See figure 2.9(a).

One might think to directly repeat the diagonalisation procedure from section 2.8, but diagonalizing the full Hamiltonian from equation (2.82) will lead to certain complications. The diagonalisation of the full Hamiltonian will give a set of vibrational states (each vibrational state with its wavefunction on the coordinate R). If considered in the continuous limit we get a discrete set of bound states and a continuous (i.e. uncountably infinite) set of free states. This kind of spectrum will likely be challenging to implement in numerical methods.

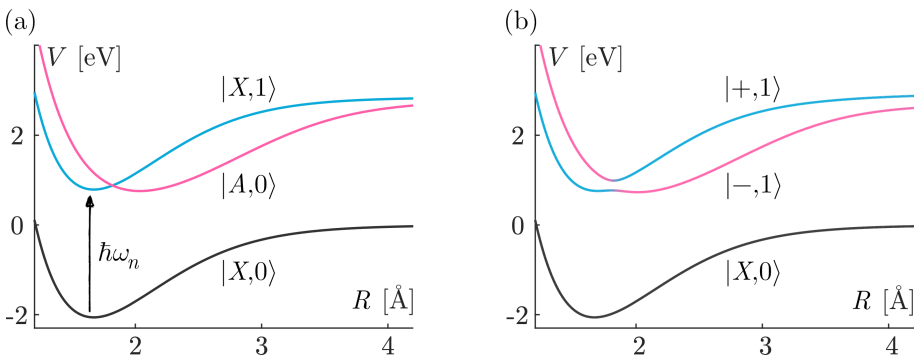

Figure 2.9: Potential energy surfaces before and after polaritonic diagonalisation. (a) The ground-state, and the first two excited states in the product basis of cavity and molecule. (b) The diagonalisation of the (partial) Hamiltonian gives polaritonic potential energy surfaces. There is a Rabi splitting in the energies at the previous intersection of the surfaces (similar to figure 2.7). The colours of the curves represent the mixture of molecular excitation in pink and cavity excitation in blue.

The reason that we get vibrational states is the kinetic energy operator, $\partial_R^2/2m$, from equation (2.82). It couples neighbouring points along R and delocalises the eigenstates. As a response, we can omit this operator and diagonalise a partial Hamiltonian pointwise (i.e. independently at each point along R). From this, we get a new set of potential energy surfaces, which are superpositions of the original ones. See figure 2.9(b). Just like we saw in figure 2.7, this mixing is due to the off-diagonal coupling elements in the Hamiltonian, $g(R)(\hat{\sigma}^\dagger\hat{a} + \hat{\sigma}\hat{a}^\dagger)$, and around the newly formed avoided crossing the potential energy surfaces are an equal parts mixture of the original ones.

As we would expect when omitting a term in the Hamiltonian before diagonalisation, the polaritonic potential energy surfaces do not represent true eigenstates of the system. Although they are often close enough to be effective as an interpretational tool. Their deviation from eigenstates becomes apparent when observing population transfer between them. This transfer comes from the omitted kinetic energy operator and predominantly takes place around the avoided crossing—where the mixture of the original states changes rapidly along R. The change in the mixture is indicated by the smooth, but sudden, change of colours in figure 2.9(b).

We will finish this section on diatomic molecules by pointing out some details that were covertly omitted. When dealing with an atom, we could omit the contribution of the nuclei, and remove diagonal matrix elements, when going from equation (2.73) to (2.74). For a diatomic molecule, the positions of the nuclei are included in the dipole moments, $\mu(R)$ (where we remember that $g := -\sqrt{2}\,\mu\,\mathcal{E}_\mathrm{c}$). Also, depending on the electronic state we get permanent dipole moments, i.e. the diagonal term we neglected for the atom. However, the permanent dipole moment will couple the cavity field to the vibrational states of the molecule, which are energetically much closer together than electronic states. Thus, assuming that the cavity mode is the fundamental one, there are no photons of lower energy to interact with these vibrational transitions in this model.

2.9.2 An emitter ensemble in the Tavis–Cummings model

In Papers I and III [1,3], a diatomic molecule is accompanied by an ensemble of atoms in the optical cavity. Modifying the Jaynes–Cummings Hamiltonian from equation (2.82) to include an ensemble of atoms is done by replacing all terms with atomic operators by sums over the entire ensemble.

$$\hat{H} = \hbar\omega_n\,\hat{a}^\dagger\hat{a} + \sum_m E_\mathrm{a}\,\hat{\sigma}_m^\dagger\sigma_m + \mu\,\mathcal{E}_\mathrm{c}\sum_m\left(\hat{\sigma}_m^\dagger\hat{a} + \sigma_m\hat{a}^\dagger\right) \tag{2.86}$$

This is the so-called Tavis–Cummings model that was first studied in 1967 [71, 72]. An important finding in such ensemble systems is the appearance of *dark*

states. They appear in the polaritonic basis, after the Hamiltonian is diagonalised, and they gain no population under Hamiltonian evolution. These dark states are discussed more in section 3.3 and in Paper III [3].

2.10 Strong coupling vs. ultra-strong coupling

In the larger field of cavity quantum electrodynamics, which encompasses polaritonic chemistry, the term *strong coupling* refers to a comparison between the light–matter coupling strength, g (in units of energy), and the rate of losses within the system [7]. This can be done by transforming a decay rate, κ, to a corresponding energy broadening, Γ. When the coupling is sufficiently large compared to the broadening, we say that we are in the *strong coupling* regime.

$$g \gg \Gamma = \hbar\kappa \qquad \Rightarrow \qquad \text{Strong coupling} \tag{2.87}$$

This is the regime where Rabi oscillations (section 2.8.1) can be observed, and the regime that the groundbreaking experiments in the eighties (section 1.2) were able to reach.

In Paper II [2], we investigate a system that crosses the boundary to strong coupling. We do this by varying the rate of photon decay.

There is a second way that is also commonly used to characterise the light–matter coupling strength. Instead of comparing with system losses, we can compare the coupling, g, with the typical energy scale in the system (also known as *bare energies* [7]). An example of this is the energy of the cavity photon, $\hbar\omega_n$, which will correspond to the energies in the relevant emitter transitions (assuming resonance). When the coupling is sufficiently large compared to the typical energy scale, we say that we are in the *ultra-strong coupling* regime.

$$g \gg \hbar\omega_n \qquad \Rightarrow \qquad \text{Ultra-strong coupling} \tag{2.88}$$

In the literature, a ratio of 10 % has often been taken as the threshold, i.e. when $g/\hbar\omega_n = 0.1$, but this is of course arbitrary and more of a historical convention [7].

In this ultra-strong coupling regime, approximations in the Jaynes–Cummings model will start to break down. The rotating wave approximation starts to lose its validity, and the Hamiltonian should include an extra term called *dipole self-energy* (not discussed in this thesis, see for instance [73]).

Because these two terms compare the coupling strength to different things, the rate of decay versus the typical energy scale, we can imagine a situation where the coupling is on the same order of magnitude as the typical energy scale, but the losses in the system are also very large. This system would counter-intuitively belong to the ultra-strong coupling regime, while not being in the strong coupling regime.

2.11 Open quantum systems

It is never practical to model a universe to understand a quantum system. In fact, stretching a fully quantum mechanical description to a single molecule can become very challenging if the molecule grows large. So in general, one makes assumptions that the system is isolated, and restricts the relevant degrees of freedom to a manageable number. For an isolated quantum system, the state, $|\psi\rangle$, is a vector in an appropriately specified Hilbert space, and its time-evolution follows the unitary evolution of the Schrödinger equation.

$$\mathrm{i}\hbar\,\partial_t|\psi\rangle = \hat{H}\,|\psi\rangle \tag{2.89}$$

Unfortunately, this formalism becomes inadequate for many situations of interest. For instance, if there is imperfect information about the state of the system and the initial state is only known as some probability distribution $\{p_i\}$ of possible initial states $\{|\psi_i\rangle\}$. Or, as we discuss in Papers II and III [2, 3], there are processes that make such a probability distribution more uncertain over time.

The pure state is not adequate to describe this situation since summing the states $\{|\psi_i\rangle\}$ with weights $\{p_i\}$ will create another pure state from an interfering superposition. We can however avoid interference effects if we take the outer product of our states, $\{|\psi_i\rangle\}$, before weighting and summing them.

$$\hat{\rho} := \sum_i p_i\,|\psi_i\rangle\langle\psi_i| \tag{2.90}$$

This is the so-called *density operator*, $\hat{\rho}$, which contains the information about the statistical probabilities of the states.

With this formalism, quantum states are no longer vectors in a Hilbert space, but, just like observables, they are operators acting on vectors in that space. The Schrödinger equation (2.89) is then generalised to the von Neumann equation (also known as the Liouville–von Neumann equation).

$$\partial_t\hat{\rho} = -\frac{\mathrm{i}}{\hbar}\big[\hat{H},\hat{\rho}\big] \tag{2.91}$$

If $\hat{\rho}$ is formed with no uncertainty about the state of the system, i.e. $\hat{\rho} = |\psi\rangle\langle\psi|$, we say that the state is pure, and with a Hermitian Hamiltonian, we can show that equation (2.91) is identical to (2.89).

This density operator formalism is then useful for the broader range of problems in *open quantum systems*; where the system is no longer assumed to be isolated, and environment interactions are included in the model. The system and its environment will then evolve as a single quantum system and build up coherences in the combined product Hilbert space. Such a state is not possible to describe with a direct sum of the individual Hilbert spaces. This implies that a state that is pure when considering the system and environment

together will be a statistical mixture when described in either of the Hilbert spaces individually. We can investigate how some open quantum system evolves by first considering a full model that contains the degrees of freedom in both the system and its environment.

Let T be the total system with state $\hat{\rho}_T$. T is then partitioned into the system that we want to study, S, and for its state we use $\hat{\rho}_S$. We call the environment B (for bath), and we will not need its density matrix. Knowing the total state, $\hat{\rho}_T$, we can get the state $\hat{\rho}_S$ by selecting a basis for B, $\{|\phi_B\rangle\}$, and summing over all matrix elements with respect to this basis. This is called a partial trace over B.

$$\hat{\rho}_S = \mathfrak{Tr}_B\big[\hat{\rho}_T\big] := \sum_{\{|\phi_B\rangle\}} \langle\phi_B|\hat{\rho}_T|\phi_B\rangle \tag{2.92}$$

Note that this formula silently implies that the inner products happen in the Hilbert space of B, and in the Hilbert space of S, $\hat{\rho}_T$ is multiplied by the identity operator. There is an important consequence of this operation; even if the total state $\hat{\rho}_T$ is pure, there is no guarantee that $\hat{\rho}_S$ will be pure, in fact, it is typically not.

An in-principle approach to then do time-evolution of $\hat{\rho}_S$ would be to time-evolve the total state $\hat{\rho}_T$ and repeatedly trace over B. But even for interactions with small environments, this is usually infeasible. A better approach is to derive a dynamical equation for $\hat{\rho}_S$ alone, from knowing just enough about the Hamiltonian of the total system [74]. One of the most popular equations from that approach is the Lindblad master equation.

$$\partial_t\hat{\rho}_S = -\frac{\mathrm{i}}{\hbar}\big[\hat{H},\hat{\rho}_S\big] + \sum_n \kappa_n\Big(\hat{L}_n\hat{\rho}_S\hat{L}_n^\dagger - \frac{1}{2}\big[\hat{L}_n^\dagger\hat{L}_n,\hat{\rho}_S\big]_+\Big) \tag{2.93}$$

Here we have used the anti-commutator $[\hat{A},\hat{B}]_+ := \hat{A}\hat{B} + \hat{B}\hat{A}$. This equation is ubiquitous because it is the most general equation that is still restricted to Markovian processes [74]; meaning that the environment has no memory of previous interactions and is essentially acting as a large reservoir.

For some basic understanding of the Lindblad equation, we first observe that the first term is simply the von Neumann equation (2.91), so essentially the Schrödinger equation in disguise. The last sum is then built from Lindblad operators $\{\hat{L}_n\}$, which are possibly non-Hermitian operators that come in two flavours; jump operators (which are non-Hermitian), and de-phasing operators (which are Hermitian).

The de-phasing operators decohere the system without changing its energy, i.e. making the state more statistically mixed. This is a way to model weak interactions with the immediate environment, where for example the environment is introducing some uncertainty in the energies of the system [75], or entanglement is built up between parts of the system and their environment [76].

The jump operators, on the other hand, will transfer population between certain states in the system, S, either by decay (where energy is lost to the

environment) or by excitation (where the system is driven). The prefactors $\{\kappa_n\}$ in equation (2.93) then modulate the rate of each process associated with any individual Lindblad operator.

In both Papers II and III [2, 3], we use the Lindblad jump operators to include photon decay in our model. And in Paper III we also use de-phasing operators to investigate the effects of populating dark states.

CHAPTER 3

Research focus

Aligned with the profile of the TQDSpec group (Molecular Quantum Dynamics and Spectroscopy) my contributions to polaritonic chemistry are theoretical investigations. Some method development has been a part of the work. For instance, eigenvector tracing in Paper I [1], reducing computational complexity in Paper II [2], and ensuring the accuracy of the dephasing operators in Paper III [3]. However, the main idea behind our work is to employ numerical simulations to explore what kind of behaviours we expect to find in polaritonic chemistry systems. The end goal is, as Fregoni et al. put it, "to build a toolbox of polaritonic phenomenologies" [25]. Our approach aims to isolate individual properties or processes, and thus characterise their influence on systems for polaritonic chemistry.

In this chapter, we address how this is achieved in practice, and we discuss the overarching motivations and goals of the research. First with a quick general view (section 3.1), then each paper is considered with a brief description of the motives, the methods, and a summary of results (sections 3.2, 3.3, and 3.4).

3.1 A challenge for theoretical models

Due to limitations in accessing the relevant time scales and spatial resolutions through experimental means, theoretical understanding and modelling have a central role to play in polaritonic chemistry [34]. There are however some approximations made in theoretical methods that can cause some gaps between theory and experiment. Here we discuss one that is of particular interest to this thesis.

A significant portion of polaritonic chemistry experiments is carried out with ensembles of emitters, which experience a collective strong coupling to the cavity mode [10]. This can be a particularly challenging system to model since there are important processes going on globally as well as with individual emitters: The individual emitters have molecular vibrations that are important for their chemical behaviour, and these are resource-demanding to model in a quantum mechanical framework. Then, the entire ensemble is collectively coupled to the cavity mode, which means that the evolution of any individual emitter depends on more than its local environment. Making accurate theoretical models in this situation has been identified as an important pursuit [12]. And some of the work in this thesis aims to approach this question [1, 3].

3.2 Paper I – Atom assisted photochemistry in optical cavities

In the Tavis–Cummings model [71,72] (i.e. the extension of the Jaynes–Cummings model beyond a single atom) it has been well established that the collective light–matter coupling strength increases with the number of two-level emitters, N. The collective coupling strength is commonly determined from the Rabi splitting of the system, ΔE_{R}.

$$\Delta E_{\mathrm{R}} = 2g\sqrt{N} = 2(\boldsymbol{\mu} \cdot \boldsymbol{\mathcal{E}}_{\mathrm{c}})\sqrt{N} \tag{3.1}$$

This Rabi splitting assumes a resonant Tavis–Cummings model (figure 2.7 shows this for a single atom). The Rabi frequency is twice the coupling strength of single emitters, g, but also scaled with the square root of the number of emitters, $\sqrt{N}$. In terms of system properties, the coupling, g, then depends on the transition dipole moments and the electric field strengths in three dimensions, $\boldsymbol{\mu}$ and $\boldsymbol{\mathcal{E}}_{\mathrm{c}}$ respectively [17,69]. Note that the Rabi splitting relates directly to the Rabi frequency from equation (2.84): $\Delta E_{\mathrm{R}} = \hbar\Omega_{\mathrm{R}}$.

The fact that the collective coupling strength increases with $\sqrt{N}$ is taken advantage of in many polaritonic chemistry experiments [10]. Here, strong coupling is achieved by having enough emitters in the cavity. However, in theoretical models, it is computationally challenging to model a large number of emitters with the state of the art quantum mechanical models. To avoid simplifications of the emitter model, one approach is to consider a single emitter (or very few) and increase the coupling strength to make up for the fact that we only model one emitter. However, it is not entirely clear what side effects there will be when many, weakly coupled, emitters are replaced with a single, but strongly coupled, emitter.

In Paper I [1] we explore a middle ground. Since quantum mechanical models of many molecules can be so expensive, we consider an ensemble that has features from polaritonic chemistry but is cheaper to model. Thus, we introduce a single diatomic MgH^+ molecule in the cavity and accompany it with an ensemble of two-level systems. We used the physical properties of the Mg atom for the two-level system, thus, they are referred to as atoms in the following.

Initially, the MgH^+ molecule is excited to an unstable electronic state. It is well known that strong coupling in cavities can stabilise an otherwise unstable molecule and that this effect becomes significant when the light–matter coupling is strong enough. Then, if a strong coupling can be substituted by many, weakly coupled, emitters, perhaps adding more atoms in the cavity will stabilise the molecule.

This turns out to be only partially correct. We set up the numerical model and ran calculations while varying both the number of atoms, N, and the

electric field strength, $\mathcal{E}_c$ (which is proportional to the coupling). The generated data shows that there is an earlier onset of molecular stabilisation when a few atoms are added to the cavity. Unfortunately, the stabilising effect is also overall suppressed the more atoms are introduced. See Paper I [1] to read more about the model and the data we produced, as well as a more detailed discussion of the results.

3.3 Paper II – Simulating photodissociation reactions in bad cavities with the Lindblad equation

Many experimental setups in polaritonic chemistry have to deal with photon decay. As discussed in section 1.1, such photon decay is particularly prevalent in the plasmonic nano-cavities.

Modelling decay effects is frequently done in the framework of open quantum systems while employing the Lindblad equation (section 2.11). This has been common practice in cavity quantum electrodynamics [16]. However, such studies are predominantly done within quantum optics and quantum information, and much less in polaritonic chemistry. That started to change in 2020 when the first few papers started to emerge [26, 77, 78]. They were able to include decay using a reduction of the Lindblad equation to a non-Hermitian evolution of a pure state. Under suitable conditions, this approach has proven to be effective while reducing the computational demand. However, if the system and observable are not ensured to be compatible with this approach, the method could simply yield inaccurate results. Thus, in 2021, publications emerged that confronted the computational challenges of the Lindblad equation head-on [79, 80], and our work from Paper II was one example [2].

We repeated much of the setup from Paper I [1]; studying the stability of the MgH^+ molecule after excitation to the same unstable electronic state, but now with no additional atoms. The photon decay rate is the primary parameter whose effect we are investigating. A second parameter is the electric field strength that, like in Paper I [1], influences the stability of the molecule in known ways (when there is no photon decay).

We set up a numerical model based on the time-evolution of the density matrix, and ran calculations while varying the electric field strength, $\mathcal{E}_c$, and the photon lifetime, τ. The generated data shows that there are two mechanisms for stabilising the molecule. The first is the well-known stabilising effect of a strongly coupled cavity with low losses. But we can also stabilise the molecule with sufficient photon decay when the excess energy is dissipated faster than the molecule can dissociate. See Paper II [2] to read more about the model and the data we produced, as well as a more detailed discussion of the results.

3.4 Paper III – Manuscript – The role of dephasing for dark state coupling in a molecular Tavis–Cummings model

Paper III [3] blends many methods and ideas from previous papers [1, 2]. We considered an ensemble of atoms and a single diatomic molecule, as in Paper I. We included photon decay and constructed the model based on open quantum systems, as in Paper II. However, several novel aspects were also introduced in this study.

In Paper III [3] we consider the diatomic CO molecule, which is a significantly more stable species than MgH^+. Thus, for this work, we study a different observable: It is well known that models with ensembles of identical emitters, such as the Tavis–Cummings model [71, 72], will have states in them that are not populated under Hamiltonian evolution, so-called *dark states*. They were present in Paper I [1] but gained no population there. In this work, we wanted to introduce physical processes to populate these states in a model for polaritonic chemistry. That process is *emitter dephasing*, which is an approximative way to include the interaction between emitters and their respective local environment. One important difference between the dark states and the regular (bright) states is that the dark ones are superpositions of excitations in only the emitters (and not the cavity field mode). Thus, if the excitation is moved into the dark state subspace it will be protected from photon decay. Our observable was therefore energy retention, and we did indeed observe the expected increase in energy retention when there are enough dark states and the dephasing rate is sufficiently high. This work highlights the importance of considering dephasing effects in polaritonic chemistry and adds to a more complete picture of the dynamics of these systems.

In contrast to Paper II [2], the inclusion of the two-level systems would not allow us to time-evolve a density matrix (section 2.11). It would simply be too large to store in memory when pushing the number of atoms towards $N_\mathrm{a} = 60$. Under these circumstances, we seized the opportunity to explore a technique known as *quantum trajectories*. This method allows us to handle systems with otherwise too memory-consuming density matrices. It is based on the technique of breaking up the statistical distribution in the density matrix on several, stochastic, time-evolutions of pure states.

See Paper III [3] to read more about the model, the quantum trajectories method, the data we produced, and a more detailed discussion of the results.

3.5 Conclusion and outlook

In this thesis, the research in polaritonic chemistry has explored emitter ensembles and also opened up the systems for environment interactions. The results provide new insights into the dynamics of these systems, which we trust can have significant implications for coming chemistry applications.

Looking ahead, there are several avenues for further investigation. One such avenue is method development for improved models of ensemble systems. The fact that bright polaritonic states are symmetric under emitter permutation [81, 82] is a potential for reduction of the size of the wavefunction. And fresh research is currently emerging that attempts to model ensemble systems based on a few molecule description [83].

Other research directions that I find particularly interesting are the questions about how to increase the accuracy of the models. The models that I work with first solve the electronic Hamiltonian, and then introduce interaction with the electric field together with the nuclear motion. However, since electrons are charged particles it is not hard to imagine that including the state of the electric field when finding the electronic eigenstates may give a different result. This is the so-called *cavity Born–Oppenheimer* approximation and our group has contributed to the research activity [84].

In conclusion, this research has provided an important early step, with new insights into the behaviour of polaritonic systems. With continued research and development, we hope polaritonic systems may someday play an important role in our toolkit for controlling chemical reactions for our benefit.

On a personal level, it has been a joy to learn the techniques and the foundational ideas for quantum mechanical models that we used for this work.

Simma lugnt!

CHAPTER 4

Bibliography

[1] E. Davidsson and M. Kowalewski, "Atom assisted photochemistry in optical cavities", The Journal of Physical Chemistry A, vol. 124, no. 23, pp. 4672–4677, 2020. https://doi.org/10.1021/acs.jpca.0c03867

[2] E. Davidsson and M. Kowalewski, "Simulating photodissociation reactions in bad cavities with the Lindblad equation", The Journal of Chemical Physics, vol. 153, no. 23, p. 234304, 2020. https://doi.org/10.1063/5.0033773

[3] E. Davidsson and M. Kowalewski, "The role of dephasing for dark state coupling in a molecular tavis–cummings model", 2023. https://arxiv.org/abs/2304.09583

[4] P. Törmä and W. L. Barnes, "Strong coupling between surface plasmon polaritons and emitters: a review", Reports on Progress in Physics, vol. 78, no. 1, p. 013901, dec 2014. https://doi.org/10.1088/0034-4885/78/1/013901

[5] J. Flick, M. Ruggenthaler, H. Appel, and A. Rubio, "Atoms and molecules in cavities, from weak to strong coupling in quantum-electrodynamics (QED) chemistry", Proceedings of the National Academy of Sciences, vol. 114, no. 12, pp. 3026–3034, 2017. https://www.pnas.org/doi/abs/10.1073/pnas.1615509114

[6] R. F. Ribeiro, L. A. Martínez-Martínez, M. Du, J. Campos-Gonzalez-Angulo, and J. Yuen-Zhou, "Polariton chemistry: controlling molecular dynamics with optical cavities", Chem. Sci., vol. 9, pp. 6325–6339, 2018. http://dx.doi.org/10.1039/C8SC01043A

[7] A. Frisk Kockum, A. Miranowicz, S. De Liberato, S. Savasta, and F. Nori, "Ultrastrong coupling between light and matter", Nature Reviews Physics, vol. 1, no. 1, pp. 19–40, Jan 2019. https://doi.org/10.1038/s42254-018-0006-2

[8] M. Hertzog, M. Wang, J. Mony, and K. Börjesson, "Strong light–matter interactions: a new direction within chemistry", Chem. Soc. Rev., vol. 48, pp. 937–961, 2019. http://dx.doi.org/10.1039/C8CS00193F

[9] K. Hirai, J. A. Hutchison, and H. Uji-i, "Recent progress in vibropolaritonic chemistry", ChemPlusChem, vol. 85, no. 9, pp. 1981–1988, 2020. https://chemistry-europe.onlinelibrary.wiley.com/doi/abs/10.1002/cplu.202000411

[10] J. Fregoni, F. J. Garcia-Vidal, and J. Feist, "Theoretical challenges in polaritonic chemistry", ACS Photonics, vol. 9, no. 4, pp. 1096–1107, 2022. https://doi.org/10.1021/acsphotonics.1c01749

[11] E. T. Jaynes and F. W. Cummings, "Comparison of quantum and semiclassical radiation theories with application to the beam maser", Proc. of the IEEE, vol. 51, no. 1, pp. 89–109, Jan 1963. https://ieeexplore.ieee.org/document/1443594

[12] M. S. Rider and W. L. Barnes, "Something from nothing: linking molecules with virtual light", Contemporary Physics, vol. 62, no. 4, pp. 217–232, 2021. https://doi.org/10.1080/00107514.2022.2101749

[13] R. Chikkaraddy, B. de Nijs, F. Benz, S. J. Barrow, O. A. Scherman, E. Rosta, A. Demetriadou, P. Fox, O. Hess, and J. J. Baumberg, "Single-molecule strong coupling at room temperature in plasmonic nanocavities", Nature, vol. 535, no. 7610, pp. 127–130, Jul 2016. https://doi.org/10.1038/nature17974

[14] J. J. Baumberg, J. Aizpurua, M. H. Mikkelsen, and D. R. Smith, "Extreme nanophotonics from ultrathin metallic gaps", Nature Materials, vol. 18, no. 7, pp. 668–678, Jul 2019. https://doi.org/10.1038/s41563-019-0290-y

[15] A. F. Koenderink, "Single-photon nanoantennas", ACS Photonics, vol. 4, no. 4, pp. 710–722, 2017, pMID: 29354664. https://doi.org/10.1021/acsphotonics.7b00061

[16] H. Mabuchi and A. C. Doherty, "Cavity quantum electrodynamics: Coherence in context", Science, vol. 298, no. 5597, pp. 1372–1377, 2002. https://science.sciencemag.org/content/298/5597/1372

[17] J. Feist, J. Galego, and F. J. Garcia-Vidal, "Polaritonic chemistry with organic molecules", ACS Photonics, vol. 5, no. 1, pp. 205–216, 2018. https://doi.org/10.1021/acsphotonics.7b00680

[18] N. A. Gippius, I. A. Shelykh, D. D. Solnyshkov, S. S. Gavrilov, Y. G. Rubo, A. V. Kavokin, S. G. Tikhodeev, and G. Malpuech, "Polarization multistability of cavity polaritons", Phys. Rev. Lett., vol. 98, p. 236401, Jun 2007. https://link.aps.org/doi/10.1103/PhysRevLett.98.236401

[19] N. M. Hoffmann, L. Lacombe, A. Rubio, and N. T. Maitra, "Effect of many modes on self-polarization and photochemical suppression in cavities", The Journal of Chemical Physics, vol. 153, no. 10, p. 104103, 2020. https://doi.org/10.1063/5.0012723

[20] S. Gambino, M. Mazzeo, A. Genco, O. Di Stefano, S. Savasta, S. Patanè, D. Ballarini, F. Mangione, G. Lerario, D. Sanvitto, and G. Gigli, "Exploring light–matter interaction phenomena under ultrastrong coupling regime", ACS Photonics, vol. 1, no. 10, pp. 1042–1048, 2014. https://doi.org/10.1021/ph500266d

[21] A. N. Lebedenko, G. Y. Guralchuk, A. V. Sorokin, S. L. Yefimova, and Y. V. Malyukin, "Pseudoisocyanine J-aggregate to optical waveguiding crystallite transition: Microscopic and microspectroscopic exploration", The Journal of Physical Chemistry B, vol. 110, no. 36, pp. 17 772–17 775, 2006, pMID: 16956261. https://doi.org/10.1021/jp061965t

[22] D. G. Lidzey, D. D. C. Bradley, T. Virgili, A. Armitage, M. S. Skolnick, and S. Walker, "Room temperature polariton emission from strongly coupled organic semiconductor microcavities", Phys. Rev. Lett., vol. 82, pp. 3316–3319, Apr 1999. https://link.aps.org/doi/10.1103/PhysRevLett.82.3316

[23] A. Graf, M. Held, Y. Zakharko, L. Tropf, M. C. Gather, and J. Zaumseil, "Electrical pumping and tuning of exciton-polaritons in carbon nanotube microcavities", Nature Materials, vol. 16, no. 9, pp. 911–917, Sep 2017. https://doi.org/10.1038/nmat4940

[24] J. Flick and P. Narang, "Cavity-correlated electron-nuclear dynamics from first principles", Phys. Rev. Lett., vol. 121, p. 113002, Sep 2018. https://link.aps.org/doi/10.1103/PhysRevLett.121.113002

[25] J. Fregoni, G. Granucci, E. Coccia, M. Persico, and S. Corni, "Manipulating azobenzene photoisomerization through strong light–molecule coupling", Nature Communications, vol. 9, no. 1, p. 4688, Nov 2018. https://doi.org/10.1038/s41467-018-06971-y

[26] S. Felicetti, J. Fregoni, T. Schnappinger, S. Reiter, R. de Vivie-Riedle, and J. Feist, "Photoprotecting uracil by coupling with lossy nanocavities", The Journal of Physical Chemistry Letters, vol. 11, no. 20, pp. 8810–8818, 2020. https://doi.org/10.1021/acs.jpclett.0c02236

[27] M. Gudem and M. Kowalewski, "Triplet-triplet annihilation dynamics of naphthalene", Chemistry – A European Journal, vol. 28, no. 40, p. e202200781, 2022. https://chemistry-europe.onlinelibrary.wiley.com/doi/abs/10.1002/chem.202200781

[28] R. C. Couto and M. Kowalewski, "Suppressing non-radiative decay of photochromic organic molecular systems in the strong coupling regime", Phys. Chem. Chem. Phys., vol. 24, pp. 19 199–19 208, 2022. http://dx.doi.org/10.1039/D2CP00774F

[29] T. Byrnes, N. Y. Kim, and Y. Yamamoto, "Exciton–polariton condensates", Nature Physics, vol. 10, no. 11, pp. 803–813, Nov 2014. https://doi.org/10.1038/nphys3143

[30] P. Lodahl, S. Mahmoodian, and S. Stobbe, "Interfacing single photons and single quantum dots with photonic nanostructures", Rev. Mod. Phys., vol. 87, pp. 347–400, May 2015. https://link.aps.org/doi/10.1103/RevModPhys.87.347

[31] X. Gu, A. F. Kockum, A. Miranowicz, Y. Liu, and F. Nori, "Microwave photonics with superconducting quantum circuits", Physics Reports, vol. 718-719, pp. 1 – 102, 2017. http://www.sciencedirect.com/science/article/pii/S0370157317303290

[32] F. Brennecke, T. Donner, S. Ritter, T. Bourdel, M. Köhl, and T. Esslinger, "Cavity QED with a Bose–Einstein condensate", Nature, vol. 450, no. 7167, pp. 268–271, Nov 2007. https://doi.org/10.1038/nature06120

[33] T. Szidarovszky, G. J. Halász, and Á. Vibók, "Three-player polaritons: nonadiabatic fingerprints in an entangled atom–molecule–photon system", New Journal of Physics, vol. 22, no. 5, p. 053001, may 2020. https://doi.org/10.1088%2F1367-2630%2Fab8264

[34] H. L. Luk, J. Feist, J. J. Toppari, and G. Groenhof, "Multiscale molecular dynamics simulations of polaritonic chemistry", Journal of Chemical Theory and Computation, vol. 13, no. 9, pp. 4324–4335, 2017. https://doi.org/10.1021/acs.jctc.7b00388

[35] F. Herrera and F. C. Spano, "Cavity-controlled chemistry in molecular ensembles", Phys. Rev. Lett., vol. 116, p. 238301, Jun 2016. https://link.aps.org/doi/10.1103/PhysRevLett.116.238301

[36] E. Cortés, W. Xie, J. Cambiasso, A. S. Jermyn, R. Sundararaman, P. Narang, S. Schlücker, and S. A. Maier, "Plasmonic hot electron transport drives nano-localized chemistry", Nature Communications, vol. 8, no. 1, p. 14880, Mar 2017. https://doi.org/10.1038/ncomms14880

[37] L. A. Martínez-Martínez, R. F. Ribeiro, J. Campos-González-Angulo, and J. Yuen-Zhou, "Can ultrastrong coupling change ground-state chemical reactions?" ACS Photonics, vol. 5, no. 1, pp. 167–176, 2018. https://doi.org/10.1021/acsphotonics.7b00610

[38] S. M. Ashrafi, R. Malekfar, A. Bahrampour, and J. Feist, "Long-distance heat transfer between molecular systems through a hybrid plasmonic-photonic nanoresonator", Journal of Optics, 2020. http://iopscience.iop.org/article/10.1088/2040-8986/abcfd6

[39] R. Juárez-Amaro, A. Zúñiga-Segundo, and H. Moya-Cessa, "Several ways to solve the Jaynes–Cummings model", Applied Mathematics and Information Sciences, vol. 9, no. 1, pp. 299–303, 2015. http://www.naturalspublishing.com/Article.asp?ArtcID=7446

[40] Y. Kaluzny, P. Goy, M. Gross, J. M. Raimond, and S. Haroche, "Observation of self-induced Rabi oscillations in two-level atoms excited inside a resonant cavity: The ringing regime of superradiance", Phys. Rev. Lett., vol. 51, pp. 1175–1178, Sep 1983. https://link.aps.org/doi/10.1103/PhysRevLett.51.1175

[41] D. Meschede, H. Walther, and G. Müller, "One-atom maser", Phys. Rev. Lett., vol. 54, pp. 551–554, Feb 1985. https://link.aps.org/doi/10.1103/PhysRevLett.54.551

[42] R. J. Thompson, G. Rempe, and H. J. Kimble, "Observation of normal-mode splitting for an atom in an optical cavity", Phys. Rev. Lett., vol. 68, pp. 1132–1135, Feb 1992. https://link.aps.org/doi/10.1103/PhysRevLett.68.1132

[43] D. M. Coles, P. Michetti, C. Clark, W. C. Tsoi, A. M. Adawi, J.-S. Kim, and D. G. Lidzey, "Vibrationally assisted polariton-relaxation processes in strongly coupled organic-semiconductor microcavities", Advanced Functional Materials, vol. 21, no. 19, pp. 3691–3696, 2011. https://onlinelibrary.wiley.com/doi/abs/10.1002/adfm.201100756

[44] S. Wang, T. Chervy, J. George, J. A. Hutchison, C. Genet, and T. W. Ebbesen, "Quantum yield of polariton emission from hybrid light-matter states", The Journal of Physical Chemistry Letters, vol. 5, no. 8, pp. 1433–1439, 2014, pMID: 26269990. https://doi.org/10.1021/jz5004439

[45] A. Shalabney, J. George, J. Hutchison, G. Pupillo, C. Genet, and T. W. Ebbesen, "Coherent coupling of molecular resonators with a microcavity mode", Nature Communications, vol. 6, no. 1, p. 5981, Jan 2015. https://doi.org/10.1038/ncomms6981

[46] A. Thomas, J. George, A. Shalabney, M. Dryzhakov, S. J. Varma, J. Moran, T. Chervy, X. Zhong, E. Devaux, C. Genet, J. A. Hutchison, and T. W. Ebbesen, "Ground-state chemical reactivity under vibrational coupling to the vacuum electromagnetic field", Angewandte Chemie International Edition, vol. 55, no. 38, pp. 11 462–11 466, 2016. https://onlinelibrary.wiley.com/doi/abs/10.1002/anie.201605504

[47] D. M. Coles, N. Somaschi, P. Michetti, C. Clark, P. G. Lagoudakis, P. G. Savvidis, and D. G. Lidzey, "Polariton-mediated energy transfer between organic dyes in a strongly coupled optical microcavity", Nature Materials, vol. 13, no. 7, pp. 712–719, Jul 2014. https://doi.org/10.1038/nmat3950

[48] S. Aberra Guebrou, C. Symonds, E. Homeyer, J. C. Plenet, Y. N. Gartstein, V. M. Agranovich, and J. Bellessa, "Coherent emission from a disordered organic semiconductor induced by strong coupling with surface plasmons", Phys. Rev. Lett., vol. 108, p. 066401, Feb 2012. https://link.aps.org/doi/10.1103/PhysRevLett.108.066401

[49] G. Wendin, "Quantum information processing with superconducting circuits: a review", Reports on Progress in Physics, vol. 80, no. 10, p. 106001, sep 2017. https://doi.org/10.1088%2F1361-6633%2Faa7e1a

[50] T. Pellizzari, S. A. Gardiner, J. I. Cirac, and P. Zoller, "Decoherence, continuous observation, and quantum computing: A cavity QED model", Phys. Rev. Lett., vol. 75, pp. 3788–3791, Nov 1995. https://link.aps.org/doi/10.1103/PhysRevLett.75.3788

[51] F. G. March, "Introduction to cavity QED", 2011. https://api.semanticscholar.org/CorpusID:17063980

[52] J. I. Cirac, P. Zoller, H. J. Kimble, and H. Mabuchi, "Quantum state transfer and entanglement distribution among distant nodes in a quantum network", Phys. Rev. Lett., vol. 78, pp. 3221–3224, Apr 1997. https://link.aps.org/doi/10.1103/PhysRevLett.78.3221

[53] S. Gleyzes, S. Kuhr, C. Guerlin, J. Bernu, S. Deléglise, U. Busk Hoff, M. Brune, J.-M. Raimond, and S. Haroche, "Quantum jumps of light recording the birth and death of a photon in a cavity", Nature, vol. 446, no. 7133, pp. 297–300, Mar 2007. https://doi.org/10.1038/nature05589

[54] S. Haroche, "Nobel lecture: Controlling photons in a box and exploring the quantum to classical boundary", Rev. Mod. Phys., vol. 85, pp. 1083–1102, Jul 2013. https://link.aps.org/doi/10.1103/RevModPhys.85.1083

[55] F. H. M. Faisal, "Theory of multiphoton processes". Springer New York, NY, 1987. ISBN 9780306423178. https://link.springer.com/book/10.1007/978-1-4899-1977-9

[56] C. Schäfer, M. Ruggenthaler, V. Rokaj, and A. Rubio, "Relevance of the quadratic diamagnetic and self-polarization terms in cavity quantum electrodynamics", ACS Photonics, vol. 7, no. 4, pp. 975–990, 2020, pMID: 32322607. https://doi.org/10.1021/acsphotonics.9b01649

[57] D. M. Rouse, "The effects of strong environmental coupling on light harvesting systems", Ph.D. thesis, 2021.

[58] J. D. Jackson, "Classical electrodynamics". John Wiley & Sons, Ltd, Aug 1998. ISBN 978-0-471-30932-1. https://www.wiley.com/en-us/Classical+Electrodynamics%2C+3rd+Edition-p-9780471309321

[59] P. Norman, K. Ruud, and T. Saue, "Principles and practices of molecular properties". John Wiley & Sons, Ltd, 2018. ISBN 9781118794821. https://onlinelibrary.wiley.com/doi/abs/10.1002/9781118794821

[60] W. P. Schleich, "Quantum optics in phase space". John Wiley & Sons, Ltd, 2001. ISBN 9783527602971. https://onlinelibrary.wiley.com/doi/abs/10.1002/3527602976

[61] J. J. Sakurai and J. Napolitano, "Modern quantum mechanics". Pearson, 2014. ISBN 1-292-02410-0

[62] D. J. Griffiths and D. F. Schroeter, "Introduction to quantum mechanics". Cambridge University Press, 2018. https://doi.org/10.1017/9781316995433

[63] M. O. Scully and M. S. Zubairy, "Quantum optics". Cambridge University Press, 1997. http://doi.org/10.1017/CBO9780511813993

[64] S. Girvin, R. . Huang, A. Blais, A. Wallraff, and R. Schoelkopf, "Course 16 - Prospects for strong cavity quantum electrodynamics with superconducting circuits", ser. Les Houches. Elsevier, 2004, vol. 79, pp. 591–608. http://www.sciencedirect.com/science/article/pii/S0924809903800409

[65] F. Jensen, "Introduction to computational chemistry". 111 River Street, Hoboken, NJ 07030, USA: John Wiley & Sons, Ltd, 2006. ISBN 0470011866. https://www.wiley.com/en-us/Introduction+to+Computational+Chemistry%2C+2nd+Edition-p-9780470058046

[66] J. Larson and T. Mavrogordatos, "The Jaynes–Cummings model and its descendants", ser. 2053-2563. IOP Publishing, 2021. ISBN 978-0-7503-3447-1. https://dx.doi.org/10.1088/978-0-7503-3447-1

[67] M. Kowalewski and S. Mukamel, "Manipulating molecules with quantum light", Proceedings of the National Academy of Sciences, vol. 114, no. 13, pp. 3278–3280, 2017. https://www.pnas.org/content/114/13/3278

[68] W. Vogel and D.-G. Welsch, "A single atom in a high-Q cavity". John Wiley & Sons, Ltd, 2006, ch. 12, pp. 407–441. ISBN 9783527608522. https://onlinelibrary.wiley.com/doi/abs/10.1002/3527608524.ch12

[69] J. Galego, F. J. Garcia-Vidal, and J. Feist, "Cavity-induced modifications of molecular structure in the strong-coupling regime", Phys. Rev. X, vol. 5, p. 041022, Nov 2015. https://link.aps.org/doi/10.1103/PhysRevX.5.041022

[70] M. Kowalewski, K. Bennett, and S. Mukamel, "Non-adiabatic dynamics of molecules in optical cavities", The Journal of Chemical Physics, vol. 144, no. 5, p. 054309, 2016. https://doi.org/10.1063/1.4941053

[71] M. Tavis and F. Cummings, "The exact solution of N two level systems interacting with a single mode, quantized radiation field", Physics Letters A, vol. 25, no. 10, pp. 714–715, 1967. https://www.sciencedirect.com/science/article/pii/0375960167909577

[72] M. Tavis and F. W. Cummings, "Exact solution for an N-molecule—radiation-field Hamiltonian", Phys. Rev., vol. 170, pp. 379–384, Jun 1968. https://link.aps.org/doi/10.1103/PhysRev.170.379

[73] V. Rokaj, D. M. Welakuh, M. Ruggenthaler, and A. Rubio, "Light–matter interaction in the long-wavelength limit: no ground-state without dipole self-energy", Journal of Physics B: Atomic, Molecular and Optical Physics, vol. 51, no. 3, p. 034005, jan 2018. https://dx.doi.org/10.1088/1361-6455/aa9c99

[74] D. Manzano, "A short introduction to the Lindblad master equation", AIP Advances, vol. 10, no. 2, p. 025106, 2020. https://doi.org/10.1063/1.5115323

[75] F. Marquardt and A. Püttmann, "Introduction to dissipation and decoherence in quantum systems", 2008. https://arxiv.org/abs/0809.4403

[76] A. C. S. Costa, M. W. Beims, and W. T. Strunz, "System-environment correlations for dephasing two-qubit states coupled to thermal baths", Phys. Rev. A, vol. 93, p. 052316, May 2016. https://link.aps.org/doi/10.1103/PhysRevA.93.052316

[77] I. S. Ulusoy and O. Vendrell, "Dynamics and spectroscopy of molecular ensembles in a lossy microcavity", The Journal of Chemical Physics, vol. 153, no. 4, p. 044108, 2020. https://doi.org/10.1063/5.0011556

[78] P. Antoniou, F. Suchanek, J. F. Varner, and J. J. Foley, "Role of cavity losses on nonadiabatic couplings and dynamics in polaritonic chemistry", The Journal of Physical Chemistry Letters, vol. 11, no. 21, pp. 9063–9069, 2020. https://doi.org/10.1021/acs.jpclett.0c02406

[79] J. Torres-Sánchez and J. Feist, "Molecular photodissociation enabled by ultrafast plasmon decay", The Journal of Chemical Physics, vol. 154, no. 1, p. 014303, 2021. https://doi.org/10.1063/5.0037856

[80] D. Wellnitz, G. Pupillo, and J. Schachenmayer, "A quantum optics approach to photoinduced electron transfer in cavities", The Journal of Chemical Physics, vol. 154, no. 5, p. 054104, 2021. https://doi.org/10.1063/5.0037412

[81] F. Herrera and F. C. Spano, "Theory of nanoscale organic cavities: The essential role of vibration-photon dressed states", ACS Photonics, vol. 5, no. 1, pp. 65–79, 2018. https://doi.org/10.1021/acsphotonics.7b00728

[82] F. J. Hernández and F. Herrera, "Multi-level quantum rabi model for anharmonic vibrational polaritons", The Journal of Chemical Physics, vol. 151, no. 14, p. 144116, 2019. https://doi.org/10.1063/1.5121426

[83] J. B. Pérez-Sánchez, A. Koner, N. P. Stern, and J. Yuen-Zhou, "Simulating molecular polaritons in the collective regime using few-molecule models", Proceedings of the National Academy of Sciences, vol. 120, no. 15, p. e2219223120, 2023. https://www.pnas.org/doi/abs/10.1073/pnas.2219223120

[84] T. Schnappinger and M. Kowalewski, "Nonadiabatic wave packet dynamics with ab initio cavity-Born-Oppenheimer potential energy surfaces", Journal of Chemical Theory and Computation, vol. 19, no. 2, pp. 460–471, 2023, pMID: 36625723. https://doi.org/10.1021/acs.jctc.2c01154

APPENDIX A

Details for calculations

A.1 Details for the interaction Hamiltonian

In section 2.3.2 we pull a phase out of the wavefunction:

$$\psi(t,\hat{\mathbf{r}}) = \mathrm{e}^{\mathrm{i}\,q(\hat{\mathbf{r}}\cdot\mathbf{A})/\hbar}\,\psi'(t,\hat{\mathbf{r}}) \tag{A.1}$$

The consequences of this are used to simplify the Hamiltonian. Here we derive these consequences.

A.1.1 Details for the transformation of operators

The time derivative transforms:

$$\mathrm{i}\hbar\partial_t\psi = \mathrm{i}\hbar\partial_t\left(\mathrm{e}^{\mathrm{i}\,q(\hat{\mathbf{r}}\cdot\mathbf{A})/\hbar}\,\psi'(t,\hat{\mathbf{r}})\right) = \tag{A.2}$$

$$= \mathrm{i}\hbar\left(\frac{\mathrm{i}q}{\hbar}(\hat{\mathbf{r}}\cdot\partial_t\mathbf{A})\,\mathrm{e}^{\mathrm{i}\,q(\hat{\mathbf{r}}\cdot\mathbf{A})/\hbar}\psi'(t,\hat{\mathbf{r}}) + \mathrm{e}^{\mathrm{i}\,q(\hat{\mathbf{r}}\cdot\mathbf{A})/\hbar}\,\partial_t\psi'(t,\hat{\mathbf{r}})\right) = \tag{A.3}$$

$$= \mathrm{e}^{\mathrm{i}\,q(\hat{\mathbf{r}}\cdot\mathbf{A})/\hbar}\big(\mathrm{i}\hbar\partial_t - q\,(\hat{\mathbf{r}}\cdot\partial_t\mathbf{A})\big)\psi'(t,\hat{\mathbf{r}}) \tag{A.4}$$

The gradient transforms:

$$\hat{\boldsymbol{\nabla}}_{\mathbf{r}}\psi(t,\hat{\mathbf{r}}) = \hat{\boldsymbol{\nabla}}_{\mathbf{r}}\left(\mathrm{e}^{\mathrm{i}\,q(\hat{\mathbf{r}}\cdot\mathbf{A})/\hbar}\,\psi'(t,\hat{\mathbf{r}})\right) = \tag{A.5}$$

$$= \mathrm{e}^{\mathrm{i}\,q(\hat{\mathbf{r}}\cdot\mathbf{A})/\hbar}\,\hat{\boldsymbol{\nabla}}_{\mathbf{r}}\psi'(t,\hat{\mathbf{r}}) + \frac{\mathrm{i}q}{\hbar}\mathbf{A}\,\mathrm{e}^{\mathrm{i}\,q(\hat{\mathbf{r}}\cdot\mathbf{A})/\hbar}\,\psi'(t,\hat{\mathbf{r}}) = \tag{A.6}$$

$$= \mathrm{e}^{\mathrm{i}\,q(\hat{\mathbf{r}}\cdot\mathbf{A})/\hbar}\left(\hat{\boldsymbol{\nabla}}_{\mathbf{r}} + \frac{\mathrm{i}q}{\hbar}\mathbf{A}\right)\psi'(t,\hat{\mathbf{r}}) \tag{A.7}$$

The Laplacian transforms:

$$\hat{\nabla}^2_{\mathbf{r}}\psi(t,\hat{\mathbf{r}}) = \hat{\nabla}^2_{\mathbf{r}}\left(\mathrm{e}^{\mathrm{i}\,q(\hat{\mathbf{r}}\cdot\mathbf{A})/\hbar}\,\psi'(t,\hat{\mathbf{r}})\right) = \tag{A.8}$$

$$= \hat{\boldsymbol{\nabla}}_{\mathbf{r}}\left(\frac{\mathrm{i}q}{\hbar}\mathbf{A}\,\mathrm{e}^{\mathrm{i}\,q(\hat{\mathbf{r}}\cdot\mathbf{A})/\hbar}\,\psi'(t,\hat{\mathbf{r}}) + \mathrm{e}^{\mathrm{i}\,q(\hat{\mathbf{r}}\cdot\mathbf{A})/\hbar}\,\hat{\boldsymbol{\nabla}}_{\mathbf{r}}\psi'(t,\hat{\mathbf{r}})\right) = \tag{A.9}$$

$$\begin{aligned} = -\frac{q^2}{\hbar^2}(\mathbf{A}\cdot\mathbf{A})\,\mathrm{e}^{\mathrm{i}\,q(\hat{\mathbf{r}}\cdot\mathbf{A})/\hbar}\,\psi'(t,\hat{\mathbf{r}}) + \frac{\mathrm{i}q}{\hbar}\mathbf{A}\,\mathrm{e}^{\mathrm{i}\,q(\hat{\mathbf{r}}\cdot\mathbf{A})/\hbar}\,\hat{\boldsymbol{\nabla}}_{\mathbf{r}}\psi'(t,\hat{\mathbf{r}}) + \\ + \frac{\mathrm{i}q}{\hbar}\mathbf{A}\,\mathrm{e}^{\mathrm{i}\,q(\hat{\mathbf{r}}\cdot\mathbf{A})/\hbar}\,\hat{\boldsymbol{\nabla}}_{\mathbf{r}}\psi'(t,\hat{\mathbf{r}}) + \mathrm{e}^{\mathrm{i}\,q(\hat{\mathbf{r}}\cdot\mathbf{A})/\hbar}\,\hat{\nabla}^2_{\mathbf{r}}\psi'(t,\hat{\mathbf{r}}) = \end{aligned} \tag{A.10}$$

$$= \mathrm{e}^{\mathrm{i}\,q(\hat{\mathbf{r}}\cdot\mathbf{A})/\hbar}\left(\hat{\nabla}^2_{\mathbf{r}} + \frac{\mathrm{i}2q}{\hbar}\mathbf{A}\cdot\hat{\boldsymbol{\nabla}}_{\mathbf{r}} - \frac{q^2}{\hbar^2}\mathbf{A}^2\right)\psi'(t,\hat{\mathbf{r}}) \tag{A.11}$$

A.1.2 Details for transforming the Schrödinger equation

We insert the transformations from section A.1.1 into the Schrödinger equation (2.22), using the Hamiltonian from equation (2.32). Since all the identical phase factors are on to the left in equations (A.4), (A.7), and (A.11) these are removed before we begin.

$$\mathrm{i}\hbar\partial_t\psi(t,\mathbf{x}) = \left(\frac{1}{2m}\left(-\hbar^2\hat{\nabla}_{\mathbf{r}}^2 + \mathrm{i}2\hbar q\mathbf{A}\cdot\hat{\boldsymbol{\nabla}}_{\mathbf{r}} + q^2\mathbf{A}^2\right) + q\Phi\right)\psi(t,\mathbf{x}) \tag{A.12}$$

$$\longrightarrow \tag{A.13}$$

$$\begin{aligned}(\mathrm{i}\hbar\partial_t - q(\hat{\mathbf{r}}\cdot\partial_t\mathbf{A}))\,\psi(t,\mathbf{x}) = \\ = \left(\frac{1}{2m}\Bigg(-\hbar^2\left(\hat{\nabla}_{\mathbf{r}}^2 + \frac{\mathrm{i}2q}{\hbar}\mathbf{A}\cdot\hat{\boldsymbol{\nabla}}_{\mathbf{r}} - \frac{q^2}{\hbar^2}\mathbf{A}^2\right) + \right. \\ \left. +\mathrm{i}2\hbar q\mathbf{A}\cdot\left(\frac{\mathrm{i}q}{\hbar}\mathbf{A} + \hat{\boldsymbol{\nabla}}_{\mathbf{r}}\right) + q^2\mathbf{A}^2\Bigg) + q\Phi\right)\psi(t,\mathbf{x})\end{aligned} \tag{A.14}$$

$$\Rightarrow$$

$$\begin{aligned}\mathrm{i}\hbar\partial_t\psi(t,\mathbf{x}) = \left(\frac{1}{2m}\Bigg(-\hbar^2\hat{\nabla}_{\mathbf{r}}^2 - \mathrm{i}2q\hbar\mathbf{A}\cdot\hat{\boldsymbol{\nabla}}_{\mathbf{r}} + q^2\mathbf{A}^2 - \right. \\ \left. -2q^2\mathbf{A}^2 + \mathrm{i}2\hbar q\mathbf{A}\cdot\hat{\boldsymbol{\nabla}}_{\mathbf{r}} + q^2\mathbf{A}^2\right) + q\Phi + q(\hat{\mathbf{r}}\cdot\partial_t\mathbf{A})\Bigg)\psi(t,\mathbf{x})\end{aligned} \tag{A.15}$$

$$\Rightarrow$$

$$\mathrm{i}\hbar\partial_t\psi(t,\mathbf{x}) = \left(\frac{-\hbar^2}{2m}\hat{\nabla}_{\mathbf{r}}^2 + q\Phi + q(\hat{\mathbf{r}}\cdot\partial_t\mathbf{A})\right)\psi(t,\mathbf{x}) \tag{A.16}$$

A.2 Details for cavity quantisation

These are the explicit expressions for the electric and magnetic fields:

$$\begin{cases} \mathbf{E}_n^{\perp}(t,z) = \mathbf{e}_x \sqrt{\dfrac{2}{\epsilon_0 V}}\,(\partial_t q)\sin(k_n z) \\ \mathbf{B}_n(t,z) = \mathbf{e}_y\, k_n \sqrt{\dfrac{2}{\epsilon_0 V}}\, q(t)\cos(k_n z) \end{cases} \tag{A.17}$$

where

$$k_n = \frac{\omega_n}{c} = \frac{\pi n}{L} \quad ; \quad n \in \mathbb{N}_1 \quad ; \quad z \in [0, L] \tag{A.18}$$

Inserted in the classical Hamiltonian, after which the expression is simplified.

$$H = \frac{\epsilon_0}{2}\int_V \mathbf{E}^2 + c^2\mathbf{B}^2 \,\mathrm{d}V \tag{A.19}$$

$$\begin{aligned} H = \frac{\epsilon_0}{2}\int_V (\mathbf{e}_x \cdot \mathbf{e}_x)\frac{2}{\epsilon_0 V}\big(\partial_t q\big)^2 \sin^2(k_n z) + \\ + (-\mathbf{e}_y \cdot -\mathbf{e}_y) k_n^2 c^2 \frac{2}{\epsilon_0 V}\, q^2(t)\cos^2(k_n z)\,\mathrm{d}V \end{aligned} \tag{A.20}$$

$$H = \frac{1}{V}\int_V \big(\partial_t q\big)^2 \sin^2(k_n z) + k_n^2 c^2\, q^2(t)\cos^2(k_n z)\,\mathrm{d}V \tag{A.21}$$

$$H = \frac{1}{V}\int \mathrm{d}x \int \mathrm{d}y \int_0^L \big(\partial_t q\big)^2 \sin^2(k_n z) + \omega_n^2 q^2(t)\cos^2(k_n z)\,\mathrm{d}z \tag{A.22}$$

Here we define the integration along x and y as the *mode area*, A.

$$H = \frac{A}{V}\left(\big(\partial_t q\big)^2 \int_0^L \sin^2(k_n z)\,\mathrm{d}z + \omega_n^2\, q^2(t)\int_0^L \cos^2(k_n z)\,\mathrm{d}z\right) \tag{A.23}$$

As specified by equation (A.18), the z integrals run over a whole number of periods of the trigonometric functions, which simplifies their evaluation.

$$H = \frac{A}{V}\left(\big(\partial_t q\big)^2 \frac{L}{2} + \omega_n^2\, q^2(t)\frac{L}{2}\right) \tag{A.24}$$

The volume of the cavity, $V = AL$, is by definition the *mode volume* that was used to normalise the mode functions in section 2.5.

$$H = \frac{1}{2}\Big(\big(\partial_t q\big)^2 + \omega_n^2 q^2(t)\Big) \tag{A.25}$$

Note how changing the spatial mode shape—i.e. how the field strength is geometrically arranged and falls off towards the boundaries of the optical

cavity—will only affect the numerical evaluation of what is defined as the *effective mode volume*, V [60].

A.3 Details for the Born–Oppenheimer approximation

When it is infeasible to work with a representation of the full wavefunction, $\Psi(\mathbf{R}, \mathbf{r})$, we split the Hamiltonian into a nuclear part, and an electronic part, such that the electronic degrees of freedom can be solved for first. The electronic part of the Hamiltonian is derived here.

In slight contrast to the argument in section 2.7.1, here we consider the continuous limit of $\{\mathbf{R}^i\}$. The state $|\Psi\rangle$ can then be described by these two wavefunctions, $\psi(\mathbf{R})$ for the nuclei, and for the electrons $\phi_{\mathbf{R}}(\mathbf{r})$ takes the continuous value of $\mathbf{R}$ as a parameter.

$$|\Psi\rangle = \int_{\mathbf{R},\mathbf{r}} \Psi(\mathbf{R}, \mathbf{r}) \; |\mathbf{R}, \mathbf{r}\rangle \; \mathrm{d}\mathbf{R}_1 \cdots \mathrm{d}\mathbf{R}_{N_\mathrm{n}} \mathrm{d}\mathbf{r}_1 \cdots \mathrm{d}\mathbf{r}_{N_\mathrm{e}} \tag{A.26}$$

$$\Rightarrow$$

$$|\Psi\rangle = \int_{\mathbf{R}} \psi(\mathbf{R}) \, |\mathbf{R}\rangle \otimes \left(\int_{\mathbf{r}} \phi_{\mathbf{R}}(\mathbf{r}) \, |\mathbf{r}\rangle \, \mathrm{d}\mathbf{r}_1 \cdots \mathrm{d}\mathbf{r}_{N_\mathrm{e}} \right) \mathrm{d}\mathbf{R}_1 \cdots \mathrm{d}\mathbf{R}_{N_\mathrm{n}} \tag{A.27}$$

We need not express the basis explicitly, and this relation collapses to a simple expression in terms of wavefunctions.

$$\Psi(\mathbf{R}, \mathbf{r}) = \psi(\mathbf{R}) \, \phi_{\mathbf{R}}(\mathbf{r}) \tag{A.28}$$

This is reminiscent of separation of variables, but by letting $\phi_{\mathbf{R}}(\mathbf{r})$ depend on the nuclear coordinates $\mathbf{R}$, in a parametric sense, it will be possible to represent any function $\Psi(\mathbf{R}, \mathbf{r})$.

The question is whether it is possible to determine the electronic wavefunctions $\{\phi_{\mathbf{R}^i}(\mathbf{r})\}$ without any knowledge about the state that the nuclear degrees of freedom occupy. The answer will turn out to be that this is possible under a particular approximation, which constitutes a central part of the Born–Oppenheimer approximation. To demonstrate this we introduce the full Hamiltonian, $\hat{H}$, and let it operate on the wavefunction from equation (A.28).

The Hamiltonian contains kinetic energy for the nuclei and the electrons, potential energy from Coulomb interactions between nuclei and electrons, as well as in between nuclei and electrons themselves.

$$\hat{H} = \hat{T}_\mathrm{n} + \hat{T}_\mathrm{e} + \hat{V}_\mathrm{ne} + \hat{V}_\mathrm{nn} + \hat{V}_\mathrm{ee} \tag{A.29}$$

In the same order, and expressed in the position basis, these operators have the following explicit form, when setting the electron charge and mass to one, $q_\mathrm{e} = m_\mathrm{e} = 1$.

$$\begin{aligned}\hat{H} = &-\sum_n \frac{1}{2M_n}\hat{\nabla}^2_{\mathbf{R}_n} - \sum_e \frac{1}{2}\hat{\nabla}^2_{\mathbf{r}_e} - \\ &-\sum_n\sum_e \frac{Z_n}{\left|\hat{\mathbf{R}}_n - \hat{\mathbf{r}}_e\right|} + \sum_n\sum_{\nu>n}\frac{Z_n Z_\nu}{\left|\hat{\mathbf{R}}_n - \hat{\mathbf{R}}_\nu\right|} + \sum_e\sum_{\epsilon>e}\frac{1}{\left|\hat{\mathbf{r}}_e - \hat{\mathbf{r}}_\epsilon\right|}\end{aligned} \tag{A.30}$$

We wish to solve the eigenvalue equation $\hat{H}\Psi(\mathbf{R},\mathbf{r}) = E\Psi(\mathbf{R},\mathbf{r})$, thus we insert the five Hamiltonian terms and use the separated wavefunction from equation (A.28). From the explicit form of each term, in equation (A.30), we can determine which part(s) of $\psi(\mathbf{R})\,\phi_{\mathbf{R}}(\mathbf{r})$ they operate on.

$$\begin{aligned}&\hat{H}\Big(\psi(\mathbf{R})\,\phi_{\mathbf{R}}(\mathbf{r})\Big) = \\ &= \hat{T}_{\mathrm{n}}\Big(\psi(\mathbf{R})\,\phi_{\mathbf{R}}(\mathbf{r})\Big) + \psi(\mathbf{R})\Big(\hat{T}_{\mathrm{e}}\,\phi_{\mathbf{R}}(\mathbf{r})\Big) + \\ &+ \hat{V}_{\mathrm{ne}}\Big(\psi(\mathbf{R})\,\phi_{\mathbf{R}}(\mathbf{r})\Big) + \Big(\hat{V}_{\mathrm{nn}}\,\psi(\mathbf{R})\Big)\phi_{\mathbf{R}}(\mathbf{r}) \;+\; \psi(\mathbf{R})\Big(\hat{V}_{\mathrm{ee}}\,\phi_{\mathbf{R}}(\mathbf{r})\Big)\end{aligned} \tag{A.31}$$

Most terms are self-explanatory, but the first term (with $\hat{T}_{\mathrm{n}}$) and the third term (with $\hat{V}_{\mathrm{ne}}$) require a closer look, beginning with the former. The derivatives with respect to the nuclear coordinates will act on both the nuclear and electronic wavefunctions, since they both contain a dependence on $\mathbf{R}$, albeit, for the electronic wavefunctions its $\mathbf{R}$-dependence is parametric. Nevertheless, how the total wavefunction $\Psi(\mathbf{R},\mathbf{r})$ will vary with $\mathbf{R}$ also depends on how $\phi_{\mathbf{R}}(\mathbf{r})$ varies. We employ the product rule twice.

$$\begin{aligned}&\sum_n \frac{1}{2M_n}\hat{\nabla}^2_{\mathbf{R}_n}\Big(\psi(\mathbf{R})\phi_{\mathbf{R}}(\mathbf{r})\Big) = \\ &= \sum_n \frac{1}{2M_n}\Big(\Big(\hat{\nabla}^2_{\mathbf{R}_n}\psi(\mathbf{R})\Big)\phi_{\mathbf{R}}(\mathbf{r}) + \\ &+2\Big(\hat{\boldsymbol{\nabla}}_{\mathbf{R}_n}\psi(\mathbf{R})\Big)\cdot\Big(\hat{\boldsymbol{\nabla}}_{\mathbf{R}_n}\phi_{\mathbf{R}}(\mathbf{r})\Big) + \psi(\mathbf{R})\Big(\hat{\nabla}^2_{\mathbf{R}_n}\phi_{\mathbf{R}}(\mathbf{r})\Big)\Big)\end{aligned} \tag{A.32}$$

The Born–Oppenheimer approximation suggests that the change in the electronic wavefunction is comparatively small as we vary the nuclear coordinate and the same for the second derivative. Thus we can neglect these terms.

$$\begin{cases}\hat{\boldsymbol{\nabla}}_{\mathbf{R}}\,\phi_{\mathbf{R}}(\mathbf{r}) := \mathbf{0} & \text{(A.33a)}\\ \hat{\nabla}^2_{\mathbf{R}}\,\phi_{\mathbf{R}}(\mathbf{r}) := 0 & \text{(A.33b)}\end{cases}$$

$$\Rightarrow$$

$$\hat{T}_{\mathrm{n}}\Big(\psi(\mathbf{R})\,\phi_{\mathbf{R}}(\mathbf{r})\Big) = \Big(\hat{T}_{\mathrm{n}}\,\psi(\mathbf{R})\Big)\phi_{\mathbf{R}}(\mathbf{r}) \tag{A.34}$$

We have thus removed a coupling in the Hamiltonian that would otherwise require $\psi(\mathbf{R})$ and $\phi_{\mathbf{R}}(\mathbf{r})$ to be determined simultaneously. This makes sure that nuclear and electronic degrees of freedom are decoupled, and the nuclear kinetic energy, $\hat{T}_{\mathrm{n}}$, only operates on the nuclear wavefunction $\psi(\mathbf{R})$.

The third term from equation (A.31), $\hat{V}_{\mathrm{ne}}(\psi(\mathbf{R})\,\phi_{\mathbf{R}}(\mathbf{r}))$, clearly couples the two coordinates. But we can exploit the diagonal nature of the operator, by rewriting $\psi(\mathbf{R})$ as a superposition of delta-functions.

$$\psi(\mathbf{R}) = \int_{\mathbf{R}'} \psi(\mathbf{R}')\,\delta(\mathbf{R}-\mathbf{R}')\,\mathrm{d}\mathbf{R}' \tag{A.35}$$

$$\Rightarrow \;\cdots\; \Rightarrow$$

$$\hat{V}_{\mathrm{ne}}(\mathbf{R})\Big(\psi(\mathbf{R})\,\phi_{\mathbf{R}}(\mathbf{r})\Big) = \int_{\mathbf{R}'} \psi(\mathbf{R}')\,\delta(\mathbf{R}-\mathbf{R}')\hat{V}_{\mathrm{ne}}(\mathbf{R}')\,\phi_{\mathbf{R}'}(\mathbf{r})\,\mathrm{d}\mathbf{R}' \tag{A.36}$$

Thus, we can first determine $\hat{V}_{\mathrm{ne}}(\mathbf{R}')\,\phi_{\mathbf{R}'}(\mathbf{r})$ for fixed values of $\mathbf{R}'$ and then take a superposition of these energies.

Last, we insert the integral representation from equation (A.27) in equation (A.31) and simplify the expression.

$$\begin{aligned}\hat{H}\Big(\psi(\mathbf{R})\,\phi_{\mathbf{R}}\Big) &= \Big(\hat{T}_{\mathrm{n}}\,\psi(\mathbf{R})\Big)\phi_{\mathbf{R}} + \\ &+\int_{\mathbf{R}'} \psi(\mathbf{R}')\,\delta(\mathbf{R}-\mathbf{R}')\Big(\hat{T}_{\mathrm{e}}\phi_{\mathbf{R}'} + \hat{V}_{\mathrm{ne}}(\mathbf{R}')\phi_{\mathbf{R}'} + \hat{V}_{\mathrm{nn}}(\mathbf{R}')\phi_{\mathbf{R}'} + \hat{V}_{\mathrm{ee}}\,\phi_{\mathbf{R}'}\Big)\mathrm{d}\mathbf{R}'\end{aligned} \tag{A.37}$$

In the expression above, the last parenthesis is what is called the electronic Hamiltonian, here shown in the continuous limit, but for computational purposes, we select some finite number of molecular geometries and convert the integral into a sum.